THE NATURE OF YOUNG SOLAR-TYPE STARS

FRANCOIS MÉNARD
Canada-France-Hawaii Telescope Corporation, PO Box 1597, Kamuela, HI 96743, USA
Laboratoire d'Astrophysique, Observatoire de Grenoble, UMR 5571 CNRS/UJF, BP 53, F-38041 Grenoble cedex 9, France

AND

CLAUDE BERTOUT
Institut d'Astrophysique de Paris, 98bis Boulevard Arago, F-75014 Paris, France

1. Introduction

We focus in this review on the properties of optically visible, young stellar objects (YSOs). We hope we will not be accused of undue anthropocentric reasoning if we say that these stars have an activity level compatible with their youth. Although each of these stars may display its own spectroscopic and photometric variability pattern at various wavelengths – which makes them fascinating objects to observe – they share enough basic properties to appear as classes of stars. We go through these various classes and their historical definitions in the following section. We then briefly address the question of their age; i.e., how do we know that they are young pre-main sequence stars? The rest of the review is devoted to the physical picture that has emerged over the last decade, focusing mainly on the physics of light variability, disk properties, and accretion. In each of these topics, we emphasize areas where we expect rapid progress in the next few years.

1.1. YOUNG SOLAR-TYPE STARS: THE DIFFERENT FLAVORS

The main reference catalog for young stellar objects is the unpublished Herbig and Bell catalog [86], which provides a census of Orion population emission-line objects in nearby star-forming regions. In the following, we focus on the various classes of solar-type stars in this sample.

1.1.1. *T Tauri Stars*

Classical T Tauri Stars (CTTSs). Alfred H. Joy discovered "a new type of variable stars whose prototype is T Tauri" [94], based on the following criteria: irregular light variations of about three magnitudes, spectral type F5-G5 with emission lines resembling the solar chromosphere, low luminosity, and association with dark or bright nebulosity. Joy gave a list of eleven stars and added "These stars differ from other known variables, especially in their low luminosity and the high intensity of bright H and K [Ca lines] in their spectra". None of these original stars has actual spectral type in the range F5-G5; instead they range from K to M. This illustrates the difficulties involved in classifying T Tauri stars (TTSs), especially when using low-resolution spectrograms. Selection criteria for TTSs were refined by Herbig [84] who defined the class of TTSs in terms of optical spectroscopic properties, first of all hydrogen and calcium line emission. Herbig also noted that stars with the above spectral properties are all irregular variables, and are all associated with nebulosity, which makes two of Joy's original criteria redundant. The youth of TTSs was recognized first by Ambartsumian [3], and it took a few years before this idea met with recognition in the rest of the world.

YY Orionis Stars. The term YY Orionis star was introduced by Walker [157], [158] to define the subclass of CTTSs that display inverse P Cygni absorption components at the edge of their Balmer and CaII emission lines. These absorption components are red-displaced by typically 300km s^{-1}, which is a direct indication that circumstellar matter is accreting onto the star at close to free-fall velocity. The YY Orionis phenomenon seemed at first restricted to CTTSs which have a strong UV excess in their spectral energy distribution. Appenzeller [5] then found that about 75% of the YY Orionis stars show a sizable UV excess while the same is true for only around 50% of all CTTSs. More recently, high-resolution spectroscopy of a large CTTS sample revealed that inverse P Cygni profiles are present in most CTTSs in at least one of their Balmer lines, though they appear much shallower than in YY Orionis stars ([50], [120], [118]). Thus the phenomenon of inverse P Cygni profiles seems to be rather ubiquitous in CTTSs, and one may doubt that YY Orionis characteristics are defining a peculiar class of young stellar objects. Nevertheless the question of why YY Orionis red-displaced absorption lines are much deeper than in CTTSs still remains.

Weak-Emission Line T Tauri Stars (WTTSs). Stars which obey Herbig's spectroscopic selection criteria are now called "classical" TTSs. They were discovered mainly during Hα surveys and they harbor (among other characteristics mentioned above) strong Balmer line emission, with Hα equivalent width (EW) larger than 10Å. In more recent years, another population of visible solar-type young stars that had escaped detection so far was discovered because of their strong X-ray emission ([159], [54], [160]). The basic criteria for selection of these objects are: late-type spectrum, Hα emission with EW smaller than about 10Å, LiI λ6707 absorption with EW > 0.1Å, and association with nebulosity. Because they display little activity in the optical range, and notably no line emission except for weak Hα emission, these objects are named Weak-emission line T Tauri Stars (WTTSs). The relative abundances of CTTSs and WTTSs in nearby star-forming regions is still a matter of controversy, caused in good part by the recent discovery by ROSAT of a population of X-ray active late-type stars that often have the properties given above but are found outside of star-forming regions, i.e., they are not associated with nebulosity (see §1.2.1).

The Current Paradigm for TTSs. A consensual physical picture of TTSs emerged in the late 80s. The activity of WTTSs is believed to be entirely of magnetic nature. Their rotation rates are quite large compared to the Sun ($v_{eq} \sim$ 10-20 km/s), presumably generating a strong dynamo which amplifies the stellar magnetic field, leading to strong and variable X-ray emission, flaring at short optical wavelengths, and formation of large, cool spots. All these properties - which are also seen in other fast-rotating late-type stars such as the RS CVn - will be discussed in the following sections, but we want to emphasize here that there is no apparent need to assume any other physical process for explaining the properties of WTTSs. CTTSs, on the other hand, are also magnetically active stars but they are surrounded by, and interacting with, a circumstellar, dusty accretion disk that results, together with the star, from the gravitational collapse of a rotating cloud core. The interaction region is currently thought to be the interface between disk and stellar magnetosphere, and accretion of disk matter onto the star is likely chanelled by the stellar magnetic field, resulting in localized (hot) accretion spots at the stellar surface. The interaction region is also thought to be the base of the observed collimated T Tauri wind, although the exact mechanism driving this wind is still a matter of speculation (see the reviews by Shu and Reipurth in this volume). Some CTTSs, presumably the youngest, are also surrounded by a remnant protostellar envelope, which feeds the circumstellar accretion disk. While the IR and sub-mm spectral energy distribution gives indications about physical conditions in the circumstellar disk and envelope, the main accretion diagnostics are in the optical and UV range: the spectral "veiling" - an extra-photospheric blue/UV continuum superimposed on the optical spectrum - is a measure of the accretion power, as is the Balmer jump, seen in emission in accreting CTTSs.

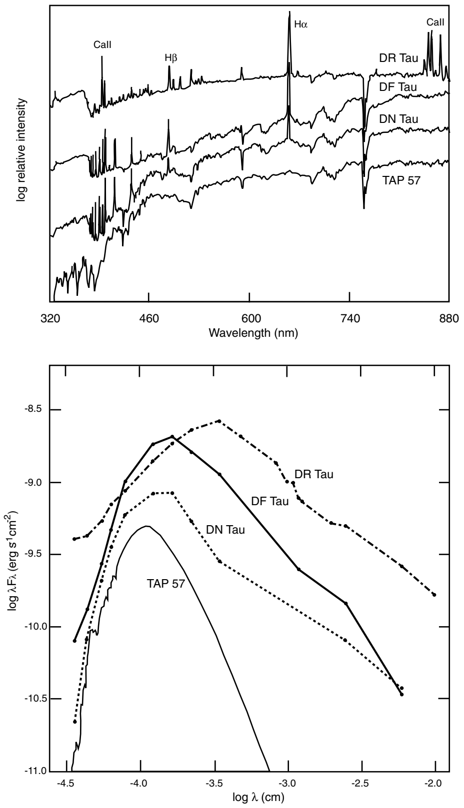

Figure 1. **Top Panel:** Medium resolution spectrograms that illustrate the variety of spectra that TTS can exhibit, ranging from the basically normal late-type spectrum of TAP57, a WTTS, through moderate CTTSs, such as DN Tauri and DF Tauri that show Balmer and Ca II emission and varying amounts of veiling , to extreme CTTSs – here DR Tauri – that displays no photospheric spectrum but many emission lines of HeI, CaII, TiII, and FeII. **Bottom Panel:** Spectral Energy Distributions of the same stars, showing the increasing infrared excess from WTTS to extreme CTTS. Note that these data were not corrected for extinction.

1.1.2. *FU Ori Stars*

This class of eruptive young objects was introduced by Herbig [85]. On the basis of one pre-outburst spectrogram of V1057 Cygni showing a spectrum characteristic of strong emission-line CTTSs, it is assumed that FU Orionis stars are in fact CTTSs undergoing a strong luminosity outburst (see also Section 2.2). Their post-outburst spectral type appears to depend on the wavelength range used for the spectral classification. For V1057 Cyg, an early A type of fairly high luminosity is derived from the blue spectral range, whereas the red range shows an approximate F5 II spectrum. Spectrograms of V1057 Cyg obtained during subsequent years show a slow decline of effective temperature and luminosity. Five years after the outburst, Herbig classified V1057 Cyg as G2-5 Ib,II in the red spectral region. Herbig [85] pointed out that each T Tauri star must undergo about one hundred FU Ori events in its lifetime of about one million years, based on the (conservative) assumption that the three observed outbursts (in FU Orionis, V1057 Cygni, and V1515 Cygni) represent all FU Ori events which occurred within 1 kpc of the Sun in the last eighty years. Properties of FU Orionis stars and their relevance to the formation of low-mass stars are discussed elsewhere in this volume by Kenyon. There have been many attempts to model FU Orionis eruptions, and a consensual picture has emerged in which the eruptive events are caused by instabilities in the circumstellar disk, leading to phases of increased accretion. Because of the high mass accretion rate, the disk brightness overwhelms the star's and the spectral signatures mentioned above trace the temperature gradient in the accretion disk.

1.2. THE CASE FOR STELLAR YOUTH

Star formation is widely thought to occur in molecular clouds, which provide the raw material from which stars can accumulate during the course of the gravitational collapse. While many details of the star formation process remain topics of controversy, the idea that most YSOs should be physically associated with molecular clouds remained unchallenged until recently.

Four main arguments are used to infer pre-main sequence status of a solar-type star: association with OB associations (e.g., in the Orion Trapezium region); association with dark or bright nebulosity (e.g., in the Taurus-Auriga region); location above the main-sequence in the Herzsprung-Russell Diagram (HRD); presence in the spectrum of the λ6707Å LiI resonance line, since this element is destroyed early in the star history.

1.2.1. *Association with OB Associations and Molecular Clouds*

The first two criteria for youth are straightforward: OB associations are short-lived, which guarantees the youth of associated low-mass objects, and physical association of a star with a cloud is either seen at the telescope when close reflection and emission nebulae are present – as is the case in the vicinity of many CTTSs – or inferred from kinematic studies (e.g., [93]).

However, it was recently argued from ROSAT data that a population of X-ray active pre-main sequence stars – many of which were identified as WTTSs – extend far beyond the boundaries of known star-forming regions (e.g.,[122],[123]). This result was at first taken as an indication that young stellar objects could migrate far away from the region of their putative formation. Propositions to explain this fact included the formation of stars in fast-moving molecular cloudlets [53] or tidally-induced escapes in multiple system members [8]. However, the recent finding that many of these PMS objects are likely the low-mass counterpart of the Gould Belt OB associations ([69],[70]) reconciles the ROSAT results with the conventional idea that these stars formed in now dispersed molecular clouds.

Another observation which may contradict the hypothesis that YSOs and molecular clouds are associated was reported by Favata et al. [52]. These authors assert, on the basis of the Hipparcos satellite astrometric

TABLE 1. Distances to the Taurus cloud and to associated young stars

Taurus	π_w	σ_w	distance (pc)
Distance indicators	6.78	0.46	147^{+11}_{-9}
Young stars	7.21	0.57	139^{+12}_{-10}
Young stars (constrained)	6.94	0.58	144^{+13}_{-11}

measurements [90], that some CTTSs of the Taurus-Auriga star-forming region are apparently much closer than previously thought and may not belong to the Taurus clouds. It was shown recently [18], however, that the TTSs observed by Hipparcos are in fact at distances compatible with their location in associated molecular clouds, and that the variability and faintness of some CTTSs conspire in some cases to induce large errors in the Hipparcos parallax determination. Table 1 gives an example of Hipparcos results relevant to the Taurus-Auriga region. There, the first line indicates the weighted average parallax π_w (with its standard error σ_w) of the Taurus cloud distance indicators discussed by [132] and [51], the second line gives the weighted average parallax of the young stars observed by Hipparcos in the Taurus-Auriga region, and the third line indicates the average parallax obtained after solving the astrometric equations while constraining all Taurus YSOs to be located at the same distance. Obviously, all these parallaxes are fully compatible, indicating that young stars are indeed at the distance of their associated molecular cloud (cf. [18] for details).

1.2.2. *Location in the HRD and Lithium Abundance*

The last two criteria for youth are more indirect. First, the location of a given star in the HRD depends on the assumption made about the respective luminosities of photosphere and circumstellar matter in a given object [97], as well as on the detailed history of how matter was accreted onto the star. However, none of these effects is expected to change drastically the location of the TTSs above the main sequence, although these are critical issues when trying to derive precise ages and masses for these objects ([126],[139],[140]). Second, the lithium abundance may be dependent on other variables than age (e.g., [154]), and the depletion of lithium during the pre-main evolution of low-mass objects is not entirely understood yet. However, the ^{7}Li abundances derived from line profile analysis of CTTSs and WTTSs in their Hayashi evolutionary phase are generally consistent with the interstellar lithium abundance, indicating that the temperature has not yet reached $2\ 10^6 K$ in the central regions of the stars (cf. [147],[11],[104],[107]).

After this brief introduction to TTSs and related objects, we turn to a more detailed analysis of their photometric variability, which is a topic of much current work.

2. The Nature of TTS Photometric Variability

2.1. HISTORICAL BACKGROUND

Stars associated with nebulosities were known to be variable before they were recognized as young stellar objects. They were classified according to the type of photometric variability they exhibited. With the introduction of independent classifications based on spectroscopic properties, interesting situations occurred; for example, the star T Tauri is a RW Aurigae variable, and RW Aurigae is a T Tauri star. In 1933, Paranego called RW Aurigae variables those irregular variable stars that belong to spectral class G and show rapid (up to one magnitude in several hours) and large (up to 3 or 4 magnitudes) variations of their brightness. Orion Nebula type variables denote those RW Aurigae variables that are associated with diffuse nebulae. In 1949, Hoffmeister proposed to extend the term RW Aurigae variable to all stars exhibiting rapid, non-periodic fluctuations, interrupted by intervals of rest, regardless of their spectral class (but excluding novae and U Geminorum stars). Commenting on the terminology of variable stars, Hoffmeister (1957) wrote "The name T Tauri stars, which was introduced by Joy, points to certain properties of the spectra and therefore does not include all objects which might be assigned to the class on the basis of photometric behavior. Furthermore, T Tauri is photometrically not characteristic of the class". While Herbig was getting rid of references to photometry in his definition of the T Tauri class, Hoffmeister was thus trying to include all nebular variables in his definition of RW Aurigae variables. Later, Glasby [59] went the opposite way by dividing nebular variables in three distinct main categories: (i) RW Aurigae variables show rapid and totally irregular light variations, (ii) T Tauri variables display slow, small amplitude sinusoidal variations with a general tendency toward stronger variations when the star is bright, (iii) T Orionis variables show small fluctuations around maximum light with sudden, irregular fading by several magnitudes. The class of TTSs, as defined by Joy and Herbig, brings together nebular variables belonging to each of these categories. "Despite their ubiquity, the light variations of the T Tauri stars have shown no clearly distinctive group property, except that an occasional display of rapid activity has been reported for most well-studied objects." wrote Herbig in his 1962 review [84], and he dismissed Hoffmeister's classification of RW Aurigae variables on the grounds that "it has not been proven that the RW Aurigae variables as so defined are a physically significant group". This obvious conflict between photometrists and spectroscopists is a thing of the past; every bit of information is useful to help us unravel the nature of these stars.

2.2. LONG-TERM VARIABILITY

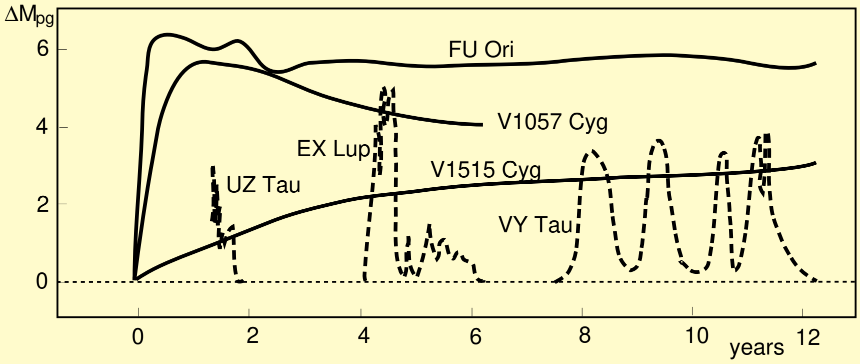

Figure 2. Compared photographic light curves of FU Orionis objects with extreme TTSs (UZ Tau, EX Lup, VY Tau), adapted from Herbig (1977).

The FU Orionis stars, briefly defined above, are characterized by a large increase in brightness over several hundred days, followed by a long-term luminosity decline. This is illustrated in Fig. 2, where the light curves of three FU Orionis objects are compared to light curves of a few TTSs with particularly large light variations such as EX Lup (from [85]). These large amplitude long-term variations are believed to be caused by disk instabilities leading to non-steady accretion ([13],[14]), with the accretion rate changing by several orders of magnitude (typically from 10^{-7} to 10^{-4} $M_{\odot}/yr$).

2.3. MID-TERM VARIABILITY

Our understanding of the mid-term (from a few days to about two weeks) variability of TTSs has progressed largely over the last decade. This resulted most notably from several multi-telescopes observing campaigns (e.g. [24], [23]) as well as from an effort by Bill Herbst and collaborators [88] to gather all available photometric data in an homogeneous database. These authors distinguish between three types of mid-term variability. It is revealing of the progress made over the last 30 years that the definitions of the first two types refer to the physical model underlying the variability rather than to the phenomenology of the light variations, in contrast to previous photometric classifications. The third variability type, on the other hand, is still largely defined on a phenomenological basis; this reflects our current lack of understanding of this particular pattern of variations. We summarize these findings below, and discuss briefly some current work on these issues. The reader is referred to the excellent discussion in [88] for details.

2.3.1. *Type I: Rotational Modulation Caused by Cold Magnetic Spots*

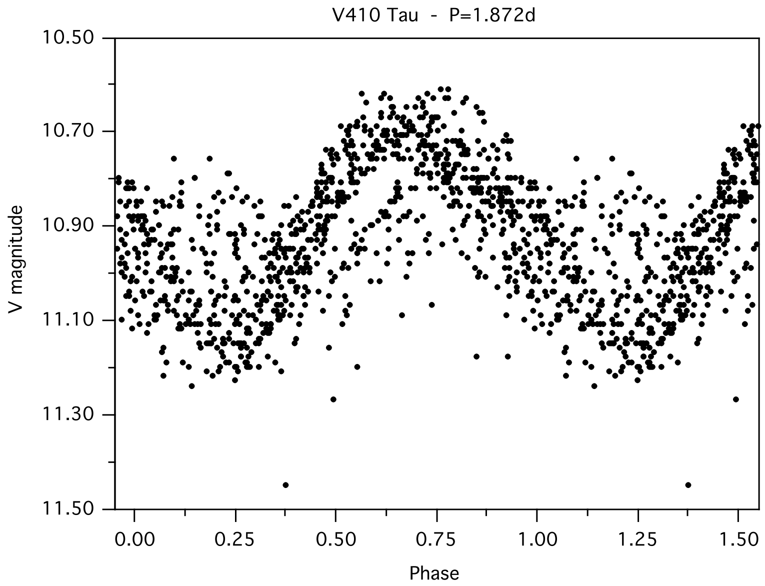

Figure 3. Phase-wrapped V-band photometric light curve for the WTTS V410 Tau, illustrating Type I periodic light variations due to dark magnetic spots on the stellar surface. The period used here is 1.872 days.

These periodic variations are seen in all young solar-type stars, but are most easily detectable in WTTSs, because it is the dominant mid-term variability cause in these stars. Figure 3, which displays all V data points available for the WTTS V410 Tau, illustrates this type of variations. The constancy of the 1.872 day period over the last 15 years is apparent on the figure, as well as some changes in the phase. While the overall spot structure remained surprisingly constant over the last 15 years, as witnessed by the nearly constant amplitude of the modulation, there are year to year changes in the shape of the light curve which reflect corresponding changes in the spot distribution and properties. The spots are often located at high-latitude in these stars, cover up to 40% of the projected surface, and are typically 1000K cooler than the remaining photosphere (see the instructive Doppler images of V410 Tau in [83] and [134]). In WTTSs, a single source of variability (the rotation of stars with cool spots) is sufficient to account for V, R, and I data. In U and sometimes B, short-term magnetic flaring is observed(e.g., [66]), especially when the stars are faint (this is similar to what is observed in dMe flare stars). The maximum amplitude that can be attributed to cold magnetic spots is about 0.8 mag in V and 0.5 mag in I.

2.3.2. *Types II and IIp: Variability Caused by Cold and Hot Spots*

Type II variations are either irregular or periodic, in which case they are called Type IIp. Both kinds of Type II variations, which occur only on CTTSs, can be understood in terms of a changing mix of cool and hot spots on their surfaces (e.g., [156],[155]). The localized hot zones on the stellar surface are attributed to accretion onto the star of circumstellar disk matter and also produce the spectroscopic veiling characteristic of the CTTS class. They are probably shorter-lived than the cold magnetic spots and can produce much larger amplitude variations (several magnitudes), particularly in the B and U filters, because of the temperatures of typically $7\ 10^3$ - 10^4K reached in the accretion zones. However, the rise time for the amplitude variations is longer and smoother than for the flares described in the previous section.

The geometry and distribution of these zones remain unclear, although first tries at CTTS Doppler imaging appear promising (e.g.,[152]). Simple spot models indicate that the stellar fraction covered by hot spots is small, typically 1% or less. However, photometric observations of YY Ori [20] revealed a quasi-periodic modulation of its light curve indicating an accretion spot covering about 10% of the stellar disk surface, i.e., much larger than hot spots usually found in CTTSs. A comparison of YY Ori's characteristics to those of CTTSs shows that YY Ori has a much larger accretion rate than usually found in CTTSs [75], suggesting a link between the accretion spot size and the accretion rate. Further comparison of the spot luminosities and accretion luminosities of a small sample of CTTSs (including YY Ori) indicated that the spot's luminosity derived from the photometric variability is much smaller than the accretion luminosity of these stars. This and the fact that the accretion rates of CTTSs with no apparent accretion spots are similar to those of CTTSs with hot spots led [20] to suggest that a sizable fraction of the accretion power might be dissipated in axially or spherically symmetric regions that do not give rise to well-defined periodicities in the light-curve. This result also has important implications regarding the nature of the accretion process, as will be discussed in the next section.

Type IIp "periodic" variability remains somewhat mysterious, because the detected periods are apparently not stable: for instance, the period seen in DN Tau varied from 6.6 days in one observing run to 8.4 days in another [24]. Similarly for DF Tau, which was observed with periods ranging from 7.5 to 8.5 days. There have been several tentative explanations (e.g., [24], [151]) but none of them appears entirely convincing. Clearly, the mechanism which leads to these period changes is a key to understanding

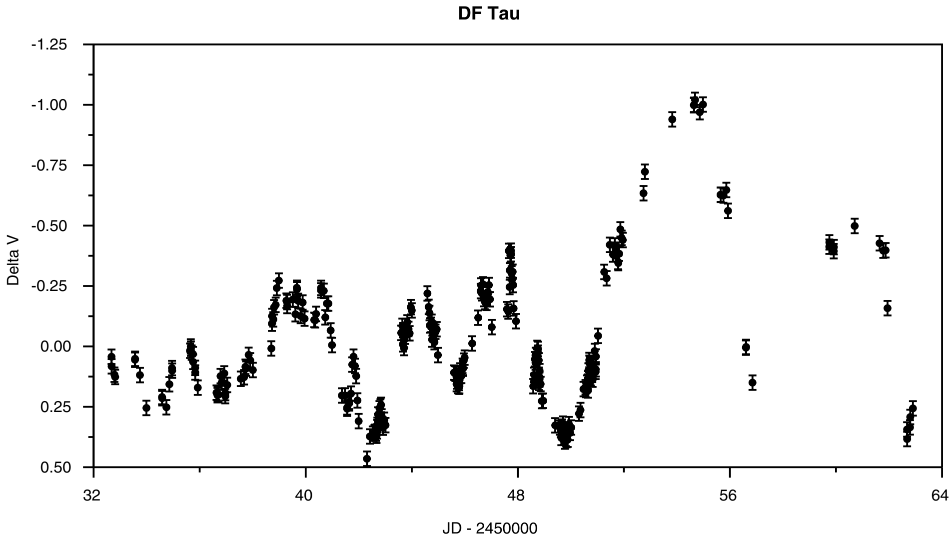

Figure 4. V-band photometric light curve of DF Tau in November 1995, illustrating Type IIp light variations due to a changing mix of cold and hot spots. See text for details.

the exact nature of the accretion process in CTTSs, and future work in this area should be rewarding. A fine example of Type IIp variability is shown in Figure 4, obtained by [33] and [26]. The periodogram of this time series shows two significant peaks at 7.45 and 4.0 days, and significant high-frequency variability is apparent in the data set. A possible model of DF Tau's light curve assumes that there are at least two accretion spots on the star and that variable accretion leads to the varying amplitudes seen in the Figure ([33] present a different interpretation).

2.3.3. *Type III: Variable Obscuration by Circumstellar Dust?*

This is the least understood variability type. It occurs mainly in Herbig Ae stars, the so-called UX Ori stars after the prototype, but also in stars with early K spectral types such as RY Tau and RY Lupi. It is characterized by large amplitude variations on stars with no evident veiling or effective temperature variations. The fact that the degree of linear polarization increases as the star fades is a major argument supporting the suggestion that variable obscuration is responsible for the star's fading. The pros and cons of the different models leading to such variability are discussed in some details by [88] and won't be repeated here. One should note, however, that Type III variability might also be present in some CTTSs with late spectral-types, most notably AA Tau [26] and possibly UY Aur [109], both of K7 spectral type [71], in contrast to previous findings[1].

[1]Note also that T Tau itself displays all three types of variability, and thus appears as a true prototype of the class [88].

2.3.4. *Are There Other Mid-Term Variability Components?*
While it is often assumed that Type I and II variabilities are enough to explain the mid-term photometric behavior of WTTSs and most late-type CTTSs, very little is known about possible variations on time-scales intermediary between the stellar rotation period (typically one week) and the slow trends observed over several years, which are thought to relate to long-term fluctuations in the accretion process. The cycle of variability in Type III objects, while not stricly periodic, recurs nevertheless on a preferred time-scale of typically 10-40 days. Herbst et al. [88] noted that this is hardly compatible with the idea that an obscuring object located in the disk causes the variability, but the timescale they considered is that of a blob crossing the stellar disk, which is probably not relevant here. Motivated by the recurrence of the observed time-scales in Type III objects, one might hypothetize instead that the relevant timescale is that of keplerian rotation within the disk, and that the obscuring objects are in fact located at distances in the range 10-20 stellar radii. The argument that the disk must be seen almost edge-on in order to get obscuration of the star by disk matter is valid only is the disk is flat, thin, and homogeneous. Instead of this idealized case, we might well have disk warps due to tidal interactions with companions, local flaring due, e.g., to anisotropic heating by radiation from the accretion spots, and density waves triggered by non-axisymmetric instabilities. All of these phenomena might lead to variability, either through partial, time-dependent obscuration of the star, or through anisotropic effects in the reprocessing of stellar light by disk matter. Whatever the mechanism leading to light variations - there has been no investigation of these effects so far - there is little reason at this point to dismiss the possibility of mid-term light variations which might give us information on physical processes at play in the inner circumstellar disk.

The problem is to detect these variations in spite of the shorter-term light variability on various timescales, which introduces a large scatter in any longer term time-series. To illustrate this point, we take a closer look at RW Aur, one of the best-studied CTTSs and a typical Type II variable. The periodogram of the V data available for this object reveals its extreme variability on all timescales, and it appears hopeless to use a periodogram analysis - a very useful tool for studying the WTTS periods - to say something about preferred timescales in RW Aur. But luckily RW Aur was one of the program star of the Hipparcos satellite, which happened to observed the star at a time when it displayed a clear periodicity.

The top panel of Figure 5 shows this time-series (black dots), which indicates a period of about 3.1 days[2]. Other Hipparcos observations (open

[2] Herbig [84] noted a preferred photometric time-scale of 5.5 days for this star. Period variations by 20% or more are commonly observed in CTTSs.

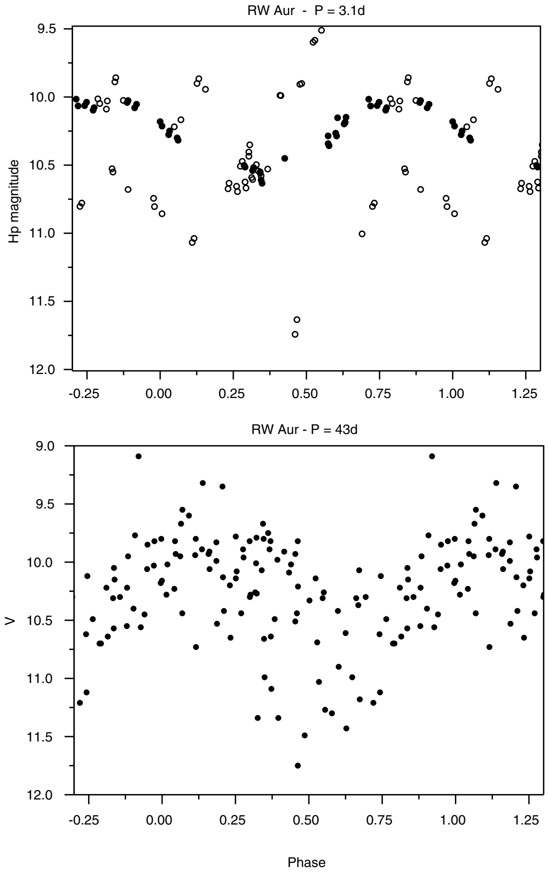

Figure 5. Variability of the CTTS RW Aur. **Top Panel:** Phase-folded Hipparcos satellite observations of RW Aur, using a period of 3.1d. The ordinate is the Hipparcos magnitude Hp. Black dots indicate a time-series of consecutive observations over more than 4 days. **Bottom Panel:** Phase-folded V data (compiled by W. Herbst) during the same time interval, showing a putative 43 day period uncovered by robust periodogram analysis. See text for details.

dots) were performed over time intervals too short to uncover a periodic behavior on the same time-scale but the phase-folded data (Fig.5) shows that the 3.1 day period was a preferred time-scale in the Hipparcos observing period, from about JD 2447900 to 2449100.

Both the amplitude of the 3.1d variations and the cycle's average magnitude vary in time, suggesting a modulation at longer time-scale. It was thus tempting to look at the large amount of UBV data obtained from the ground by various groups during the same time frame. Using a powerful period-search technique borrowed from geophysics, another preferred variation time-scale of about 43 days is uncovered in these data, as seen in the bottom panel of Fig.5, but no 3.1 day periodicity is apparent in the V data. The origin of this putative modulation is not known at present, but a full analysis of RW Aur's photometric data is currently under way [17]. In conclusion, one might say that the picture of CTTS variability is probably somewhat more complex than believed today, and is of potential interest to get information about physical conditions in the inner circumstellar disk.

2.4. SHORT-TERM VARIABILITY

Haro [73] discovered a number of flare stars in the Orion Nebula and in the Taurus-Auriga star-forming region. He called these objects flash stars in order to distinguish them from the UV Ceti stars. According to Haro [73], necessary criteria for classifying variables as flare stars are: (a) relative steadiness of the starlight during minima or "normal phase" and (b) a sudden, unpredictable rise to maximum and a slower, but still rapid, decline toward minimum. Haro classified as flash stars a number of TTSs by using his usual technique for discovering new flare stars, which consisted in repeatedly photographing the same sky region while shifting slightly the photographic plate between two exposures. A change in brightness on a time-scale of about 10 minutes is easily detected in this way. Well-known CTTSs which were classified as flash stars on the basis of one observed flare include YY Ori, NS Ori, SU Ori, as well as DF Tau, DS Tau and DN Tau. Haro in fact estimated that 30% of the Orion flare stars were also TTSs. As early as 1954, Ambartsumian speculated that TTSs were permanently flaring stars while Haro and Chavira proposed in 1955 that flash stars were post-TTSs (see [74]). None of these interpretations now appears likely.

Early UV/optical broad-band flaring observations often suffered from inadequate time coverage. It is currently believed ([58], [66], [65]) that strong ($\geq 0\overset{m}{.}3$ in all wavebands) and rapid ($\leq$ 1h with sharp rise-time and slower decay time) variations are actually rare events on TTSs. Gahm et al. [58] emphasize that the normal short-term behavior of TTSs is to be completely constant in brightness or to vary slowly with small amplitudes over several hours. Rare but powerful rapid variations may be split in two categories: flare-like energetic bursts ($10^{33} - 10^{34}$ erg) in the Balmer continuum and line emission, and smoother, slower changes (with energies up to several 10^{35} erg) seen in all broad-band filters (such as those seen on a 2h time-scale in DF Tau - cf. Fig. 4). The latter short-term variations are likely caused by veiling variations in CTTSs, i.e., by an accretion related process (see [56]) and/or by type III variations (see [58] for details) while the Balmer continuum/line flares are likely to be genuine magnetic flares as seen in dMe stars. H_α-flares might also be associated with mass-loss events, further increasing the similarities between TTS and solar-like flares of magnetic origin. The X-ray and Radio variability also support this view.

Average X-ray luminosities for TTSs, both CTTSs and WTTSs, are typically a thousand times larger than the solar one. Repeated observations showed that flares are frequent. Monitoring of the ρ Ophiuchi region lead Montmerle et al. [117] to nickname the dark cloud an "*X-ray Christmas Tree*" due to the blinking of the low-mass PMS stars above and below Einstein's detection threshold.

During flares, the electron density ($n_e \sim 10^{10} cm^{-3}$), the plasma temperature ($T \sim 10^7$ K), and the magnetic field ($B_* \sim 10^3$G) are fairly similar to values found in solar flares. The probable causes for this large luminosity is therefore the availability of a large coronal volume, or of very large loop sizes (sometimes comparable to the stellar radius!). As for the Sun, radio emission is also expected from the large magnetic loops. And, similarly to X-rays, strong variability and large radio flares were detected on TTS using the VLA (e.g., [55],[143],[21]).

2.5. CONCLUSIONS

At least two distinct physical mechanisms are playing a role in YSO photometric variations. Magnetic fields are present on the surface of all late-type YSO. Their strengths appear compatible with expectations based on the rotation rates of other late-type dwarfs, and lead to the formation of large-sized magnetic spots and hot plages, leading to: (i) mid-term periodic light variations in the visual and near-infrared range; these are observed in both WTTSs and CTTSs; (ii) short-term UV/optical variability in WTTSs and CTTSs; and (iii) X-ray emission and variability in WTTSs and CTTSs.

The second well-documented physical process leading to variability is accretion of matter by the star from its circumstellar disk. This process is likely responsible for (i) the long-term eruptions in FU Ori objects, leading to an increased stellar effective temperature by a factor of almost 2 and a brightening of the star by several magnitudes, (ii) the mid-term periodic and more erratic optical light variations in CTTSs, due to the presence on the stellar surface of short-lived accretion spots that modulate the light curve, and (iii) the short-term veiling variability on CTTSs.

There is evidence that a third physical process is at work in some CTTSs and earlier-type objects, but its nature remains elusive today. While variable obscuration of the star by circumstellar matter is likely the source of this variability, many questions about the origin of the obscuring matter, its location in the star-disk-wind system, and the timescales involved remain unanswered today.

3. The Physics of CTTS Accretion Disks

The discussion of variability above provided us with some useful insight in the accretion process: its anisotropy, as witnessed by the hot accretion spots, and its non-stationarity, revealed by the short- and mid-term optical and UV variability. What is still lacking, however, is a physical picture connecting the large-scale processes in the accretion disk to the small-scale processes taking place on the stellar surface. In other words, how does the accretion of disk matter onto the star really proceed? This is the topic of this section, where we shall review the observational evidence and accretion models after giving some historical background information.

3.1. HISTORICAL BACKGROUND

Compelling observational evidence that rotationally supported disks exist around TTSs is only recent. In his pioneering observational study of YY Orionis stars, Walker [157] was first to propose disk accretion as a possibility to explain the inverse P Cygni profiles and strong UV excess displayed by these objects. When Lynden-Bell & Pringle (LBP; [103]) suggested, in their insightful theoretical paper of 1974, that viscous dissipation in a disk might account for the continuous excesses observed in TTSs, there was basically no data available to support, or refute, this hypothesis. Observations were restricted at that time to medium resolution optical spectroscopy and optical photometry, although the presence of a near-IR excess in some bright CTTSs had been discovered by Mendoza in 1968 [110] and was usually attributed to reprocessing of stellar photons by a dusty envelope [37]. A decade went by before two satellites provided observational means for testing LBP's model: IRAS (e.g.,[135]) in the infrared and IUE in the UV. Together with ground-based broad-band photometry, these facilities provided the data needed for an extensive study of the accretion disk model. But during the years 1974-1986, much work on TTSs focused on studies of atmospheres (e.g.,[38],[87]), winds (e.g.,[79]), as well as on studies of the infall hypothesis (e.g., [150],[161]). In a thoughtful paper, DeCampli [40] demonstrated in 1981 that the mechanism driving T Tauri winds must be extremely efficient, pointing to a magnetic origin. But his analysis also implied that a non-stellar energy source was likely needed to account for the overall energy expenditures of TTSs (wind, radiative excesses).

From 1983 on, the idea that CTTSs were surrounded by disks gained momentum steadily, starting with Cohen's paper on HL Tau [36] and the illuminating analysis of T Tauri forbidden line profiles by Appenzeller and collaborators [6], convincingly demonstrating the existence of an opaque layer (the disk) hiding the recessing part of the wind. Then came the era of SED interpretations using accretion disk models and finally the disk idea reached consensual status[3] in 1989. We should perhaps emphasize that consensus was found on the basis of converging indirect evidence rather than on firm observational facts: the first direct circumstellar T Tauri disk detections dating only a few years back.

[3]Worthy of mention is the alternative CTTS model proposed by Mitskevich & Grinin where the disk is replaced by an inhomogeneous, envelope-like medium ([116], [113],[114],[115])

Similar tests of the accretion disk hypothesis were made for all classes of solar-type YSOs at about the same time, and generally turned out to be successful. Hartmann & Kenyon ([80],[81]) convincingly argued that FU Orionis outburst were caused by massive accretion onto the central star and showed that infrared CO emission lines had the double-peaked profiles expected for a rotating flat disk. Lada & Wilking [101] surveyed the dense molecular cores of ρ Ophiuchi in the infrared and were able to classify all objects into three categories (later labelled as Class I, II, and III) according to the shape of their infrared spectral energy distribution. Adams, Lada, and Shu [2] proposed that this classification is in fact an evolutionary sequence, from embedded object to ZAMS star, an idea that still holds nowadays, although with a few modifications (see the review by Lada in this volume).

Since the Crete I meeting [100], our understanding of the accretion/ejection process, and especially the pivotal role played by the disk, has evolved considerably. Most aspects of the classical LBP disk model are being challenged on both observational and theoretical grounds. The idea that the disk is flat and homogeneous has given way to the more complex view of a warped, inhomogeneous disk in which tidal interactions (induced by close companions or by non-axisymmetric instabilities) play a major role. Similarly, the classical view that disk material is accreted onto the star via an equatorial, steady boundary layer is not necessarily accurate in the complex environment of YSOs, although high-accretion rate FU Orionis objects do show evidence for boundary layer emission [95]. One should note here that the boundary layer hypothesis has been studied in some depth in recent years, and that boundary layer properties are now much better understood than they were at the Crete I meeting. The interested reader is referred to [133], [130] and references therein. In CTTSs it turns out that the stellar magnetic field is likely sufficient to disrupt the inner accretion disk, leading to magnetically controlled accretion along the stellar field lines of at least a fraction of the accreting matter. Although this accretion scenario was proposed as early as 1988 for DF Tau [19], it has become evident in recent years that it is valid for the entire CTTS class.

In the following paragraphs we shall briefly review the disk models and discuss the pros and cons of current ideas about the accretion process, using the newest observational support. We shall not discuss in detail the role played by the disk and magnetic field in the ejection process. The reader is referred, for example, to the review by Shu in this volume.

3.2. GLOBAL DISK OBSERVABLES

There are two kinds of observable quantities in accretion disk physics: global properties of the star/disk system that are accessible through unresolved photometric and spectroscopic observations, and observables which result from direct imaging and resolved polarimetry, giving access to the disk's detailed physical structure.

The global observables of disk accretion are (i) the accretion luminosity $L_{acc} = GM_* \dot{M}_{acc}/R_*$, which can – in principle – be determined from the IR and UV excesses (see below), (ii) the maximum disk temperature $T^D_{\max} = \zeta \left[L_{acc}/\sigma R_*^2\right]^{0.25}$ which is given roughly by the wavelength of the SED maximum, and (iii) the maximum disk velocity $v_K = \sqrt{GM_*/R_*}$, which measures the profile widths for spectral lines formed in the inner disk. These three quantities depend only on the stellar radius R_*, the stellar mass M_* and the mass accretion rate $\dot{M}_{acc}$ and are thus easily determined, at least to zeroth-order. The factor ζ depends on the disk model used; it is 0.287 for the standard LBP model.

From these three quantities, we can get a first reasonable guess of the physical conditions in the disk. Let's take the example of an "average" CTTS, with $R_* = 2R_\odot$, $M_* = 0.5M_\odot$, and spectral type K7. We can rewrite the equation for L_{acc} as

$$\frac{L_{acc}}{L_*} = 0.86 \left[\frac{\dot{M}_{acc}}{10^{-7} M_\odot \mathrm{yr}^{-1}}\right] \left[\frac{M_*}{0.5M_\odot}\right] \left[\frac{R_*}{2R_\odot}\right]^{-3} \left[\frac{T_{eff}}{4000\mathrm{K}}\right]^{-4} \qquad (1)$$

and assuming that $\dot{M}_{acc} = 10^{-7} M_\odot \mathrm{yr}^{-1}$we get $T^D_{\max} \approx 2000\mathrm{K}$ and $v_K \approx 220$ km/s. We thus expect mass accretion rates $\sim 10^{-7} M_\odot \mathrm{yr}^{-1}$ to be easily detected in spectroscopic and photometric work since the accretion luminosity is then comparable to the photospheric luminosity. In practice, one can detect CTTS mass accretion rates down to 10^{-9} $M_\odot \mathrm{yr}^{-1}$ by careful spectroscopic work ([9],[71]).

We also find that the dereddened spectral energy distribution (SED) should peak around 1 μm, which is observed in many CTTSs, that the disk should be mostly molecular and will contain dust, and that the near-IR lines formed in the disk should be easily resolved, which is also verified.

While these global observables thus allow for useful first-order estimates of disk properties, one needs to go into much more detail for a precise determination of the mass-accretion rate. In particular, one needs to make assumptions about the disk structure and IR emission properties.

The IR SED is made of a stellar photospheric component and an "excess emission" component, i.e., emission above what is expected from the photosphere alone (cf. Figure 1). How closely can this be related to the accretion luminosity? In general terms, the IR excess is composed of several components, depending on the disk physical model that one has in mind. When the standard LBP disk model is adapted to the case of CTTSs, the IR luminosity emitted by the disk can be written (e.g., see [1])

$$L_{IR}^{excess} = \frac{1}{2}L_{acc} + L_{rep} \tag{2}$$

where L_{acc} is the accretion luminosity and L_{rep} is the stellar luminosity reprocessed by the disk. The reprocessed luminosity depends on the amount of starlight absorbed by the disk which, in turns, depends on the dust scale height and/or the exact geometry of the disk. In the flat, geometrically thin but optically thick, viscous accretion disks envisioned by LBP, both L_{acc} and L_{rep} yield the same observational diagnostics: the disk temperature distribution and IR SED are power laws: $T(r) \propto r^{-3/4}$, and $\lambda F_\lambda \propto \lambda^{-4/3}$.

Observations suggest that the SEDs of many CTTSs depart significantly from that predicted by standard LBP flat disks. Rydgren & Zak [136] measured an average $\lambda F_\lambda \propto \lambda^{-3/4}$ over the range 3.5–20μm for 7 CTTSs, while Rucinski [135] found $\lambda F_\lambda \propto \lambda^{-1}$ in the range 12–100 μm. As noted by several authors, however, L_{rep} is highly dependent on the assumed disk geometry, and can be substantially increased if the disk intercepts more stellar photons than a flat disk, i.e., if its flaring vertical structure (in vertical hydrostatic equilibrium, the local scale height is $\propto r^{9/8}$) is taken into account (e.g., [96], [105], [39]), or if it is warped by tidal interactions ([148],[149],[102]). Realistic flaring disks do not differ much from flat disks in their innermost parts and effects of flaring is most apparent longward of about 5μm. On the other hand, a wide range of SEDs can be fitted by warped disks, depending on the disk mass and distance of the stellar companion that causes the tidal warp.

Several other causes can modify the IR SED. If the disk is disrupted and truncated by the stellar magnetic field, or if the presence of planets in the disk induces gaps, then IR emission deficit[4] occurs ([111], [108]). Non-standard disk models such as the self-gravitating, instability-ridden disk envisioned by [141], MHD accretion/ejection structures [57] have flatter IR SEDs than LBP disks. Also, thermalization by the ambient medium [15], backscattering from a dusty envelope [121], and undetected infrared companions [16] are expected to contribute to the IR flux. So, using the IR SED alone to evaluate the mass accretion rate *in the disk* is usually impossible, except when $\dot{M}_{acc}$ is so large that L_{acc} dominates over all other IR luminosity components, so that $L_{IR}^{excess} \simeq \frac{1}{2}L_{acc}$. This is the case for FU Orionis objects.

However, the IR SED can be used in conjunction with *simultaneous* UV and optical data to constrain the mass accretion rate (e.g., [19],[9],[76]) or,

[4]However, see Boss & Yorke [22] for an alternate interpretation of "dips" in the SEDs.

alternatively, the UV/optical spectrum can be used alone to determine the mass accretion rate (e.g., [153],[75],[71]). These procedures involve additional assumptions about the physics of the interaction region between star and disk. As it turns out, separating the UV-optical excess from the true photospheric emission is not an easy task, especially if the excess is small with respect to the photospheric luminosity. Further complications come from the fact that the colors of a PMS late-type photosphere and *a fortiori* the colors of the excess are not well known, so the (large) extinction corrections to apply lead to large errors in the respective luminosities. Additional uncertainties come from the accretion geometry assumed. All these have resulted in estimation of the accretion rate that can vary by as much as a factor 10 for a given star. We shall summarize the current understanding of the complex star/disk interaction region in §3.4. We now turn to those properties of disks which are unveiled by direct imaging.

3.3. DIRECT OBSERVATIONS OF ACCRETION DISKS

In a broad sense, the observers benefit from two sources of information when trying to probe the disk structure directly. The first one is the *scattered* starlight the disk is sending back, the second one is the disk's own *thermal* emission. The scattering process occurs at the surface of an optically thick disk. At millimeter wavelengths the dust thermal emission is usually assumed optically thin, except at the very center. The CO gas may be optically thick however, depending on the line and isotope. Furthermore, at optical and near-infrared wavelengths, the grains interacting with the light are small, micron-sized at most, and likely smaller. The grains responsible for the mm continuum emission are bigger. Both approaches therefore complement each other nicely, as we will see below.

There is little doubt now that disks exist around TTSs. The images of the edge-on systems HH 30 [28] and HK Tau/c [144], the rotating gas rings around the binaries GG Tau [44] and UY Aur [45], the silhouette disks in Orion [124], are as many proofs. But these images contain much more: they contain the traces of the disk structure itself.

Models usually are simplified reproduction of nature's work. In what follows we will assume that the (parametrized) disks have axial symmetry and that quantities describing them are power-laws. For exemple, the surface density distribution, the vertical scale height, the radial temperature distribution, and the density profile can be respectively expressed by the following expressions:

$$\Sigma(r) = \Sigma_0 (r/r_o)^{-p}, \quad H(r) = H_0 (r/r_o)^{\beta}, \quad T(r) = T_0 (r/r_0)^{-q}, \tag{3}$$

$$\text{and} \quad \rho(r,z) = \rho_0 (r/r_o)^{-\alpha} \exp[-|z|^2/2H^2(r)]. \tag{4}$$

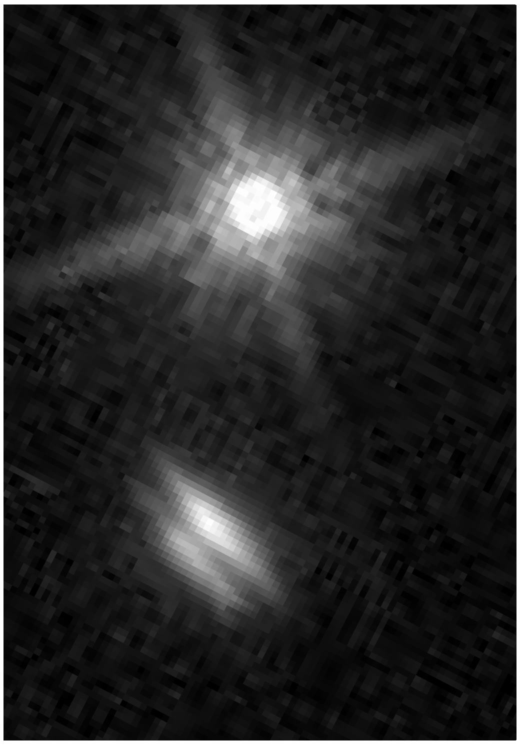

Figure 6. HST/WFPC2 image of the pre-main sequence binary star HK Tau. The F606W filter was used. It includes most of the Johnson V and R passbands. The separation between the two stars is $2''\!.4$. The companion (to the South) is entirely nebulous and the central star remains undetected at $\lambda \leq 2.2\mu$m. The dark lane is interpreted as a disk seen edge-on.

In equation (4), $\alpha \equiv p + \beta$ and we have assumed a Gaussian vertical density profile, valid for a vertically isothermal, hydrostatic, non-self gravitating disk. A summary of measured disk parameters for CTTSs is presented in Table 2 for comparison. Many of the parameters derived from the observations are best fits from multi-parameter χ^2-minimizations. Good descriptions of the dependences between the various parameters are given by, e.g., [28] for light scattering models, and by [68] for CO molecular emission models.

Outer Radius. Because the instruments have finite sensitivities, the outer radii measured are lower limits. Furthermore, a severe flaring of the disk could also cast shadow on the outer parts, reducing the amount of scattered light to zero. Nevertheless, the disks that have been imaged so far are in general *larger* than predicted by SED fitting, e.g., [12].

Whether the gaseous disk is actually larger than the dust disk remains an open issue. From existing mm-interferometric observations, one finds that either the dust disks are smaller or their emission drops below the detection limits faster (i.e., at 200-300AU) than the gas disks do (up to 850AU). However, in the case of GM Aur (a single star), UY Aur and

GG Tau (two binaries), the disks seen in scattered light extend over roughly the same distance as the CO disks. This suggests that both techniques are probing the same physical structure and the grains (at least those responsible for scattering) are mixed with the gas over large distances.

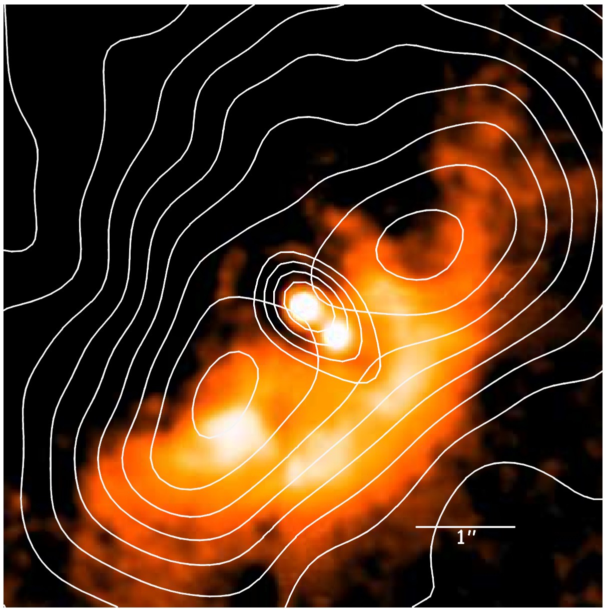

Figure 7. Overlay of the ^{13}CO $(2 \rightarrow 1)$ integrated area (large contours) and 1.3mm continuum emission (smaller contour, close to the center) over an Adaptive Optics J-band image (grey shade) obtained at CFHT. As expected if the dust and gas are well mixed, the ^{13}CO countours trace roughly the scattered light. See Close et al. (1998) for the AO image, and Duvert et al.(1998) for the radio data.

Inclination. The inclination of the disk is usually derived from the axis ratio of either the scattered light, the dust thermal continuum, or the CO gas total emission. The kinematic pattern can also be used to estimate the inclination in mm-line work. When disks are seen close to edge-on, model of the scattered light are used to estimate the inclination relying on the assumption that the nebula is uniform and both lobes should have equal brightness for $i = 90^o$. This technique has been applied for HH 30 and HK Tau/c for example.

Density Profiles and the Scale Height. For edge-on systems, H_0 can be measured directly, in principle, from optical and infrared images. However, a large flaring or a thick envelope may forbid direct view of the central parts, reducing the radial coverage and forbidding an assessment of β. A

TABLE 2. Disk parameters for CTTSs

	R_{out}^{gas} (AU)	R_{out}^{dust} (AU)	i	p	β	q	M_{disk} ($M_\odot$)	reference
HH 30	—	250	> 80	0.75	1.45	—	0.006	[28]
HK Tau/c	—	105	85	0.3–1.5	1.2	—	6×10^{-4}	[144]
GG Tau	525	> 220	43	1.5	1.25	0.5	~ 0.17	[44]
DM Tau	850	—	33	~ 1.5	1.26	0.63	≤ 0.025	[68]
UY Aur	~ 1000	> 650	42	—	—	—	≤ 0.01	[45][34]
GM Aur	525	>200	56	1.57	1.18	0.64	0.025	[43]

The values in this table are difficult to estimate. They come from the best models and observations we found. But the reader should be aware they are subject to change in the future.

wavelength coverage as wide as possible is necessary to extract a more reliable estimate. For an arbitrary inclination, estimating $\Sigma(r)$ from scattered light is difficult because the disk is optically thick. For edge-on systems, $\Sigma(r)$ and $H(r)$ are coupled (degenerate) and isolating each one is next to impossible.

However, the size of millimeter continuum sources detected in the course of a survey was modelled by Dutrey et al. [42] who concluded that the radial dependence of the surface density is probably shallower than was imagined by previous models using single dish data. This shallowness is supported by yet better models for GM Aur and DM Tau for example, see Table 2.

Temperature Profile. The results presented in Table 2 suggest that the temperature profile is flatter than 0.75, the value expected for passive or viscous but otherwise geometrically thin disks. A discussion of various possibilities leading to flatter temperature distributions has been presented in §3.2. We note however, that it is compatible with a flaring disk, as suggested by the radial dependencies of the scale height, also quoted in Table 2.

Rotation Curve. From molecular line observations, solid evidence for rotating disks have been found in a number of CTTSs now, see Table 2 but also [46] for LkCa 15, [106] for MWC 480, an Herbig Ae stars, [91] for UZ Tau E. In many cases, models showed this rotation to be consistent with Keplerian rotation, with $V(r) \propto r^{-0.5}$ within the error bars.

Disk Mass. Disk mass estimates from scattered light models are severely affected by the large optical thickness of the disk and are mere lower limits, usually. An exception to that is found, once again, in the edge-on case. Then, the optically thick disk draws a dark lane in the equatorial plane, the *thickness* of which is directly related to the disk mass. For HH 30, the mass derived from such a model agrees reasonably with the mass estimated from mm continuum flux.

Estimating disk masses from mm observations is not any easier (see, e.g., [12],[4]). One usually assumes that the dust is optically thin throughout the disk and the continuum flux therefore a good tracer of the mass. However, the grain size distribution, the dust emission properties and the dust-to-gas ratio are not well known quantities. Similarly, mass estimates based on gas phase tracers can suffer from possible optical thickness and depletion of the molecular species used. Usually, dust masses are considered more reliable because the dust opacity at 1mm is considered accurate to within a factor of a few [128] for a wide-range of grain sizes and shapes.

Assuming that a representative CTTS is 10^6 years old and that its accretion rate is $10^{-7}\mathrm{M}_\odot\ \mathrm{yr}^{-1}$, then the accreted mass is $0.1\mathrm{M}_\odot$. This is more than most of the disk masses listed in Table 2. However, the accretion rate may be lower, $10^{-8}\mathrm{M}_\odot\ \mathrm{yr}^{-1}$, and it has been shown to decline with time [78]. The mass accreted over the pre-main sequence lifetime then becomes comparable to the disk masses deduced from mm continuum emission (typically a few $0.01\mathrm{M}_\odot$), and there is no need to "feed" the original disk to sustain the accretion process. For binaries however, the situation may be different. Their disks may be smaller, with the inner disks intact, but outer disks truncated, missing. This is based on their identical NIR excess compared to single TTSs [142], but mm continuum flux lower on average ([125], [42]). This may be supported by Fig.6, where the disk of the companion in this $2\overset{''}{.}4$ binary is the smallest CTTS disk imaged so far.

3.3.1. *Concluding Remarks*

Despite the large efforts deployed by many groups, the number of resolved disks remains decivingly small, much below the fraction of 50% inferred in Taurus [146], and $\sim 70\%$ in Orion [89]. If we assume that our vision of a disk around a TTS is right (but we can also question this affirmation!) various reasons may be invoked to explain the low detection rate. Apart from the obvious limits in resolution and contrast of the instruments, grain growth and molecular gas depletion may play a role. The presence of unknown companions may also lead to truncation and destruction of the outer disks.

Asymmetries are seen in the disk of HH 30 [145], and maybe also in HK Tau/c [144]. Although their origin is not clear at present, they may indicate that the disks are rapidly evolving. Hartmann et al. [78] have also suggested that accreting disk should evolve by increasing their outer radii, hence further lowering their surface density profile. This topic of disk evolution was, however, voluntarily ignored in the present section. The reader is referred to, e.g., [146] and [142] for an overview of our knowledge of disk dissipation and survival times in single and binary CTTSs. There is no need to emphasize that a better knowledge of the disk evolution is a necessary step to future studies of planet formation.

After this review of observed disk properties, we discuss in some details the (unresolved) inner part of the disk and disk/star interaction region, where accretion takes place. At the time of the Crete I conference, hints that the accretion might be channeled by the stellar magnetic field were sparse. In the next section we discuss the changes that took place since then.

3.4. STRUCTURE OF THE STAR-DISK INTERACTION ZONE

The interface zone between the accretion disk and the central star is small enough to prevent direct imaging. Yet, it is the site of energetic and unsteady phenomena that are as many finger-prints of low-mass stellar formation. It is likely instrumental in the accretion and ejection processes, and possibly in many of the variability events discussed before. Efforts to outline its morphology and isolate the relevant mechanisms at play have been numerous. A picture of this interaction zone is slowly emerging from indirect evidence. We will describe the current supportive observational evidence in the next paragraphs, keeping in mind that this picture is likely to evolve rapidly in the years to come as the physical processes at play are complex and not completely understood.

3.4.1. *Spectro-Photometric Evidence for Magnetospheric Accretion*

The observation of inverse P Cygni profiles in hydrogen Balmer lines and permitted metallic lines with pronounced redshifted absorption is frequent in CTTSs (see §1.1.1). These features are not easily explained by a boundary layer (where accretion proceeds at subsonic speeds) but are produced naturally in magnetospheric accretion funnels [30]. Radiative transfer models adapted for this geometry can reproduce many of the observed features of various Hydrogen lines ([82],[119]), in agreement with the idea that they are formed in the accretion flow rather than in a wind[5]. In that sense, the hot spots discussed in §2.3.2 are also suggestive of accretion columns as they may trace the shocks close to the stellar surface.

The red-displaced absorption features have velocities of a few hundred km/s, suggesting infall of material along the line-of-sight at velocities close to free-fall velocity. This is compatible with a magnetosphere that connects to (and possibly truncates) the disk at a few stellar radii, close to the

[5]One should probably add a word of caution here, as line profile shapes are usually non-unique, i.e., they can be modelled using different physical models. Basic features of CTTS Balmer line profiles can also be reproduced by wind models ([99],[116]) or by other accretion scenarios ([150]).

corotation radius, and channels material along its field lines. Independent support for that view comes from the near infrared colors of CTTSs that are best explained if the inner disks are absent (truncated) over a significant fraction of the corotation radius [111]. However, see Armitage & Clarke for a caution [7].

3.4.2. *Is There an Appropriate Stellar Magnetic Field?*

The magnetospheric accretion model assumes a dipolar field, tilted or not from the stellar rotational poles, that is steady or survives long enough for accretion to get established [98]. Estimations of the magnetic field are available for a few T Tauri stars only, many of them upper limits or non-detections ([27],[60],[10],[64],[41],[67],[92]). Magnetic fields of order kG were detected in T Tau and LkCa 15([64],[67]), with large filling factors, suggesting that field-free regions are not common at the stellar surface. Using Zeeman-Doppler imaging, Donati et al. [41] showed that V410 Tau and possibly HDE 283572, two bright WTTSs, had multi-component fields, ruling out a pure dipole.

On the other hand, Johns-Krull et al. [92] did not detect a net polarization in the absorption lines of the CTTS BP Tau but they found a strong circular polarization in the HeI λ5876 *emission* line, which is presumably formed in the accretion shock. They deduced a 2.4kG field in the line formation region. This result may well be the best evidence we have so far for magnetically mediated accretion proceeding along large-scale magnetic loops, the base of which covers only a small fraction of the stellar surface.

To summarize, magnetic fields of order of 1-2 kG have been measured on a few TTSs. There are signs that the field is not steady and its geometry may not be dominantly dipolar. As such, these measurements may still be compatible with but are not proofs that magnetospheric accretion occurs.

3.4.3. *Stellar Angular Momentum Evolution*

TTSs evolving along their Hayashi tracks are spinning up because of gravitational contraction and should reach break-up velocities on a time-scale comparable with the Hayashi evolutionary phase ($\sim 10^6$yr). Additionnally, an initially slow-rotating CTTS surrounded by an accretion disk and accreting material at a rate of $\dot{\mathrm{M}} \sim 10^{-7}\mathrm{M}_\odot\mathrm{yr}^{-1}$ should reach break-up velocity on a time-scale of a few 10^4 years (e.g., [162]). In other words, if angular momentum was conserved during the Hayashi phase, all TTSs should be fast rotators, close to break-up speed. That velocities generally observed in both WTTSs and CTTSs are in the range $v \sin i$ ~10-25 km s^{-1} (about 0.1 of the break-up velocity) clearly indicates that a braking (or regulating) mechanism is efficient at confining the rotation to slow rates during the pre-main sequence phase ([98],[77]). MHD winds flowing along stellar or disk open field lines are often invoked as efficient carriers of angular momentum away from the stars (e.g., [127],[48]). However, indications that mass-loss is intimately linked to the accretion process are now available (e.g.,[29],[75]) and the disk itself could also play a determinant role in the momentum transport and spin regulation. Roughly speaking, one can imagine a scenario in which stellar field lines are anchored in the disk at or outside the corotation radius, effectively locking together the stellar and disk rotations. This idea follows from a model proposed by Gosh & Lamb, notably to explain the spin rates of pulsars ([61],[62]). Examination of the rotation periods of TTSs ([23],[49],[35]) confirmed that CTTSs are indeed slower rotators than WTTSs, and theoretical models showed that the stellar rotation could be regulated by transport of stellar angular momentum to the disk in the case of magnetic coupling ([31],[162],[32],[63],[7]).

Bouvier et al. [25] successfully modeled the evolution of angular momentum of low-mass stars with moderate and fast rotation rates from the pre-main sequence phase up to the main sequence phase. In their model, short-lived accretion disks result in main sequence stars with fast rotation because the stars are allowed to spin-up for a longer time during their contraction toward the main sequence. To the opposite, long-lived disks produce slow main sequence rotators.

From the spread of rotation periods of late-type main sequence stars, one can infer that disk lifetimes have to span a large range, from 0.1 Myr to a few 10^7yr, with a mean around 3 Myr. This is in rough agreement with disk lifetimes estimated by observations for TTSs (e.g., [146]), although 10^7yr or more may be too long (see [25] for a discussion of that issue).

3.4.4. *Problems and Prospective*

While the success of the magnetospheric accretion model to explain many observables of CTTSs is evident, Edwards [47] points out some of the weaknesses of the model. More discordantly, Safier [137] argues that there is little evidence for the long-lived, global dipole fields that are necessary in the models to insure disk truncation and steady accretion along field lines. He also shows [138] that some magnetic field detections are likely marred by systematic effects that tend to overestimate the field value. Popham [129] proposed that the angular momentum of CTTSs can be regulated by FU Orionis outbursts, and [131] discuss observational support to this hypothesis. While the angular momentum evolution models are impressive, one must note that the role of jets and winds in the angular momentum balance is not investigated in these models, in spite of its obvious relevance.

Recent 2D numerical simulations of the magnetosphere-disk interaction in fact hint at a much more complicated picture, in which various instabilities play a major role ([72], [112]). Studying several different magnetic field configurations, Miller & Stone [112] find notably that boundary layer-like, equatorial accretion occurs when the (highly time-dependent) ram pressure of the accreting material exceeds the magnetic pressure of the magnetosphere. The ram pressure depends on the angular momentum transport mechanism, which is either the Balbus-Hawley instability or magnetic braking in their simulations. They also find that the presence of a disk magnetic field comparable in strength to the stellar field itself can promote polar accretion – if the disk and stellar field are anti-aligned. They show that winds occur in all configurations they study, and that the evolution of angular momentum depends on the details of the star-disk interaction, making it difficult to predict. While this is an exploratory study that needs to be extended to a full 3D one, it is highly suggestive of the complexity of the accretion process, making it obvious that both the axisymmetric, steady boundary layer model and the dipolar magnetospheric accretion model are far too simplistic to give an accurate representation of reality.

Acknowledgements We gratefully acknowledge financial support from NATO and the Laboratoire d'Astrophysique de L'Obsevatoire de Grenoble. Thanks also to Jérôme Bouvier, Catherine Dougados, Gaspard Duchêne and Karl Stapelfeldt for their help in the preparation of this review.

References

1. Adams, F.C., Shu, F.H. 1986, ApJ, 308, 836
2. Adams, F.C., Lada, C.J., Shu, F.H. 1987, ApJ, 312, 788
3. Ambartsumian, J.R. 1947, Stellar Evolution and Astrophysics, Erevan, Acad. Sci. Armen. SSR
4. André, P., Montmerle, T. 1994, ApJ, 420, 837
5. Appenzeller, I. 1977, in *The Interaction of Variable Stars with their Environment*, eds. R. Kippenhahn, J. Rahe, and W. Strohmeier, Bamberg, Remeis-Sternwarte, p. 80
6. Appenzeller, I., Jankovics, I., Oestreicher, R. 1983, A&A, 141, 108
7. Armitage, P.J., Clarke, C.J. 1996, MNRAS, 280, 458
8. Armitage, P.J., Clarke, C.J. 1997, MNRAS, 285, 540
9. Basri, G., Bertout, C. 1989, ApJ, 341, 340
10. Basri, G., Marcy, G.W., Valenti, J.A. 1992, ApJ, 390, 622
11. Basri, G., Martin, E.L., Bertout, C. 1991, A&A, 252, 625
12. Beckwith, S.V.W., Sargent, A.I., Chini R.S., Güsten, R. 1990, AJ, 99, 924
13. Bell, K.R., Lin, D.N.C. 1994, ApJ, 427, 987
14. Bell, K.R., Lin, D.N.C., Hartmann, L.W., Kenyon, S.J. 1995, ApJ, 444, 376
15. Bell, K.R., Cassen, P.M., Klahr, H.H., Henning, Th. 1997, ApJ, 486, 372
16. Bertout, C. 1989, ARA&A, 27, 351
17. Bertout, C. 1999, in preparation
18. Bertout, C., Arenou, F., Robichon, N. 1999, A&A, submitted
19. Bertout, C., Basri, G., Bouvier, J. 1988, ApJ, 330, 350
20. Bertout, C., Harder, S., Malbet, F., Mennessier, C., Regev, O. 1996, AJ, 112, 2195
21. Bieging, J.H., Cohen, M. 1989, AJ, 98, 1686
22. Boss, A.P., Yorke, H.W. 1993, ApJ, 411, L99
23. Bouvier J., Cabrit S., Fernandez M., Martin E.L., Matthews J.M. 1993, A&AS, 101, 485

24. Bouvier, J., Cabrit, S., Fernandez, M., Martin, E.L., Matthews, J.M. 1993, A&A, 272, 176
25. Bouvier, J., Forestini, M., Allain, S. 1997, A&A, 326, 1023
26. Bouvier, J., Chelli, A., Allain, S., et al. 1999, A&A, submitted.
27. Brown, D.N., Landstreet, J.D. 1981, ApJ, 246, 899
28. Burrows, C.J., Stapelfeldt, K.S., Watson, A.M., et al. 1996, ApJ, 473, 437.
29. Cabrit, S., Edwards, S., Strom, S.E., Strom, K.M. 1990, ApJ, 354, 687
30. Calvet, N., Hartmann, L. 1992, ApJ, 386, 239
31. Cameron, A.C., Campbell, C.G. 1993, A&A, 274, 309
32. Cameron, A.C., Campbell, C.G., Quaintrell, H. 1995, A&A, 298, 133
33. Chelli, A., et al. 1999, A&A, in press
34. Close, L.M., Dutrey, A., Roddier, F. et al. 1998, ApJ, 499, 883
35. Choi, P.I., Herbst, W. 1996, AJ, 111, 283
36. Cohen, M. 1983, ApJ, 270, L69
37. Cohen, M., Kuhi, L.V. 1979, ApJ Supp, 41, 743
38. Cram, L.E. 1979, ApJ, 234, 949
39. D'Alessio, P., Canto, J., Calvet, N., Lizano, S. 1998, ApJ, 500, 411
40. De Campli, W.M. 1981, ApJ, 244, 124
41. Donati, J.F., Semel, M., Carter, B.D., Rees, D.E, Cameron, A.C. 1997, MNRAS, 291, 658
42. Dutrey, A., Guilloteau, S., Duvert, G., Prato, L., Simon, M., Schuster, K., Ménard, F. 1996, A&A, 309, 493
43. Dutrey, A., Guilloteau, S., Prato, L., Simon, M., Duvert, G., Schuster, K., M'enard, F. 1998, 338, L63
44. Dutrey, A., Guilloteau, S., Simon, M. 1994, A&A, 286, 149
45. Duvert, G., Dutrey, A., Guilloteau, S., Ménard, F., Schuster, K., Prato, L., Simon, M. 1998, A&A, 332, 867
46. Duvert, G., Guilloteau, S., Ménard, F., Simon, M., Dutrey, A. 1999, A&A, submitted
47. Edwards, S., 1997, in Proc. of IAU Symp. 182:*Herbig-Haro flows and the birth of low-mass stars*, eds. B. Reipurth and C. Bertout, Dordrecht, Kluwer, p. 433
48. Edwards, S. Mundt, R., Ray T. 1993, in *Protostars and Planets III*, eds. E.H. Levy and J.I. Lunine, Tucson, University of Arizona Press, p. 567
49. Edwards, S., Strom, S., Hartigan, P., Strom, K., Hillenbrand, L., Herbst, W., Attridge, J., Merrill, M., Probst, R., Gatley, I. 1993, AJ, 106, 372.
50. Edwards, S., Hartigan, P., Ghandour, L., Andrulis, C. 1994, AJ, 108, 1056
51. Elias, J.H. 1978, ApJ, 224, 857
52. Favata, F., Micela, G., Sciortino, S., D'Antona, F. 1998, A&A, 335, 218
53. Feigelson, E.D. 1996, ApJ, 468, 306
54. Feigelson, E.D., Jackson, J.M., Mathieu, R.D., Myers, P.C., Walter, F.D. 1987, AJ, 94, 1251
55. Feigelson, E.D., Montmerle, T. 1985, ApJ, 289, L19
56. Fernández, M., Eiroa, C. 1996, A&A, 310, 143
57. Ferreira, J., Pelletier, G. 1995, A&A, 295, 807
58. Gahm, G.F., Lodén, K., Gulbring, E., Hartstein, D. 1995, A&A, 301, 89
59. Glasby, J.S. 1974, *The Nebular Variables*, Oxford, Pergamon
60. Gnedin, Yu.N., Red'kina, N.P. 1984, Sov. Astron. Lett., 10(4), 255
61. Ghosh, P., Lamb, F.K. 1979, ApJ, 232, 259
62. Ghosh, P., Lamb, F.K. 1979, ApJ, 234, 296
63. Ghosh, P. 1995, MNRAS, 272, 763
64. Guenther, E.W. 1997, in *Herbig-Haro Flows and the Birth of Stars*, IAU Symp. No. 182, eds. B. Reipurth and C. Bertout (Dordrecht:Kluwer), p. 465
65. Guenther, E.W., Ball, M. 1999, A&A, submitted
66. Guenther, E.W., Emerson, J.P. 1997, A&A, 321, 803
67. Guenther, E.W., Lehmann, H., Emerson, J.P., Staude, J. 1999, A&A, 341, 768

68. Guilloteau, S., Dutrey, A. 1998, A&A, 339, 467
69. Guillout, P., Sterzik, M.F., Schmitt, J.H.M.M., Motch, C., Egret, D., Voges, W., Neuhäuser, R. 1998, A&A, 334, 540
70. Guillout, P., Sterzik, M.F., Schmitt, J.H.M.M., Motch, C., Neuhäuser, R. 1998, A&A, 337, 113
71. Gullbring, E., Hartmann, L., Briceño, C., Calvet, N. 1998, ApJ, 492, 323
72. Hayashi, M.R., Shibata, K., Matsumoto, R. 1996, ApJ 468, L37
73. Haro, G. 1968. in *Stars and Stellar Systems*, Vol. VII, eds. B.M. Middlehurst and L.H. Aller, Chicago, Univ. of Chicago Press, p. 141.
74. Haro, G. 1976, Bol. Inst. Tonantzintla, 2, 3
75. Hartigan, P., Edwards, S., Ghandour, L. 1995, ApJ, 452, 736
76. Hartigan, P., Hartmann, L., Kenyon, S.J., Hewett, R., Stauffer, J. 1991, ApJ Supp, 70 899
77. Hartmann, L. 1991, in *Angular momentum evolution of young stars*, eds. S. Catalano and J.R. Stauffer, NATO ASI series Dordrecht, Kluwer, p. 379
78. Hartmann, L., Calvet, N., Gullbring, E., D'Alessio, P. 1998, ApJ, 495, 385
79. Hartmann, L., Edwards, S., Avrett, A. 1982, ApJ 261, 279
80. Hartmann, L., Kenyon, S.J. 1985, ApJ, 299, 462
81. Hartmann, L., Kenyon, S.J. 1987, ApJ, 312, 243
82. Hartmann, L., Hewett, R., Calvet, N. 1994, ApJ, 426, 669
83. Hatzes, A.P. 1995, ApJ, 451, 784
84. Herbig, G.H. 1962, Advances in A&A, 1, 47
85. Herbig, G.H. 1977, ApJ, 217, 693
86. Herbig, G.H., Bell, K.R. 1988, Lick Obs. Bull. No.1111
87. Herbig, G.H., Goodrich, R.W. 1986, ApJ, 309, 294
88. Herbst, W., Herbst, D.K., Grossman, E.J., Weinstein, D. 1994, AJ, 108, 1906
89. Hillenbrand, L.A., Strom, S.E., Calvet, N., Merrill, M.K., Gatley, I., Makidon, R.B., Meyer, M.R., Skrutskie, M.F. 1998, AJ, 116, 1816
90. *The Hipparcos and Tycho Catalogues*, 1997, ESA SP-1200
91. Jensen, E.A., Koerner, D.W., Mathieu, R.D. 1996, AJ, 111, 2431
92. Johns-Krull, C.M., Valenti, J.A., Hatzes, A.P., Kanaan, A. 1999, ApJ, 510, L41
93. Jones, B.F., Herbig, G.H. 1979, AJ, 84, 1872
94. Joy, A.H. 1945, ApJ, 102, 168
95. Kenyon, S.J. 1999, this volume
96. Kenyon, S.J., Hartmann, L. 1987, ApJ, 323, 714
97. Kenyon, S.J., Hartmann, L. 1990, ApJ, 349, 197
98. Königl, A. 1991, ApJ, 370, L39
99. Kuhi, L.V. 1964, ApJ, 140, 1409
100. Lada, C.J., Kylafis, N.D. 1991, Proc. of the NATO ASI: *The Physics of Star Formation and Early Stellar Evolution*, Dordrecht, Kluwer, 746 pp.
101. Lada, C.J. 1984, Wilking, B.A. 1984, ApJ, 371, 171
102. Larwood, J.D., Nelson, R.P., Papaloizou, J.C.B., Terquem, C. 1996, MNRAS, 282, 597
103. Lynden-Bell, D. , Pringle, J.E. 1974, MNRAS, 168, 603
104. Magazzu, A., Rebolo, R., Pavlenko, I.V. 1992, ApJ, 392, 159
105. Malbet, F., Bertout, C. 1991, ApJ, 383, 814
106. Mannings, V., Koerner, D.W., Sargent, A.I. 1997, Nature, 388, 555
107. Martin, E.L., Rebolo, R., Magazzu, A., Pavlenko, Y. 1994, A&A, 282, 503
108. Mathieu, R.D., Adams, F.C., Latham, D.W. 1991, AJ, 101, 2184
109. Ménard, F., Bastien, P. 1987, in *Circumstellar Matter*, IAU Symp. 122, eds. I. Appenzeller and C. Jordan, (Dordrecht: Reidel), p. 133
110. Mendoza, V.E.E. 1968, ApJ, 151, 977
111. Meyer, M.R., Calvet, N., Hillenbrand, L.A. 1997, AJ, 114, 288
112. Miller, K.A., Stone, J.M. 1997, ApJ, 489, 890
113. Mitskevich, A.S. 1994, A&A, 281, 471

114. Mitskevich, A.S. 1995, A&A, 298, 219
115. Mitskevich, A.S. 1995b, A&A, 298, 231
116. Mitskevich, A.S., Natta, A., Grinin, V.P. 1993, ApJ, 404, 751
117. Montmerle, T., Koch-Miramond, L., Falgarone, E., Grindlay, J.E. 1983, ApJ, 269, 182
118. Muzerolle, J., Hartmann, L., Calvet, N. 1998, AJ, 116, 455
119. Muzerolle, J., Calvet, N., Hartmann, L. 1998, ApJ, 492, 743
120. Najita, J., Carr, J.S., Tokunaga, A.T. 1996, ApJ, 456, 292
121. Natta, A. 1993, ApJ, 412, 761
122. Neuhäuser, R., Sterzik, M.F., Schmitt, J.H.M.M., Wichmann, R., Krautter, J. 1995, A&A, 297, 391
123. Neuhäuser, R., Sterzik, M.F., Torres, G., Martin, E.L. 1995, A&A, 299, L13
124. O'Dell, C.R., Wen, Z., Hu, X. 1993, ApJ, 410, 696
125. Osterloh, M., Beckwith, S.V.W. 1995, ApJ, 439, 288
126. Palla, F., Stahler, S.W. 1993, ApJ, 418, 314
127. Pelletier, G., Pudritz, R.E. 1992, ApJ, 394, 117
128. Pollack, J.B., Hollenback, D., Beckwith, S., Simonelli, D., Roush, T., Fong, W. 1994, ApJ, 421, 615
129. Popham, R. 1996, ApJ, 467, 749
130. Popham, R. 1997, ApJ, 478, 734
131. Popham, R., Kenyon, S., Hartmann, L., Narayan, R. 1996, ApJ, 473, 422
132. Racine, R. 1968, AJ, 73, 233
133. Rekowski, M.v., Froehlich, H.-E., 1997, A&A, 319, 225
134. Rice, J.B., Strassmeier, K.G. 1996, A&A, 316, 164
135. Rucinski, S.M. 1985, AJ, 90, 2321
136. Rydgren, A.E., Zak, D.S. 1987, PASP, 99, 141
137. Safier, P.N. 1998, ApJ, 494, 336
138. Safier, P.N. 1999, ApJ, 510, 127
139. Siess, L., Forestini, M., Bertout, C. 1997, A&A, 326, 1001
140. Siess, L., Forestini, M., Bertout, C. 1999, A&A, 342, 480
141. Shu, F.H., Tremaine, S., Adams, F.C., Ruden, S.P. 1990, ApJ, 358, 495
142. Simon, M., Prato, L. 1995, ApJ, 450, 824
143. Stine, P.C., Feigelson, E.D., André, P., Montmerle, T. 1988, AJ, 96, 1394
144. Stapelfeldt, K.R., Krist, J.E., Ménard, F., Bouvier, J., Padgett, D.L., Burrows, C.J. 1998, ApJ, 502, L65
145. Stapelfeldt, K.R., Watson, A.M., Burrows, C.J., Krist, J.E. 1998, BAAS, 193, 1706
146. Strom, S.E. 1995, RevMexAA (serie de Conferencias), 1, 317
147. Strom, K.M., Wilkin, F.P., Strom, S.E., Seaman, R.L. 1989, AJ, 98, 1444
148. Terquem, C., Bertout, C. 1993, A&A, 274, 291
149. Terquem, C., Bertout, C. 1996, MNRAS, 279, 415
150. Ulrich, R.K. 1976, ApJ, 210, 377
151. Ultchin, Y., Regev, O., Bertout, C. 1997, ApJ, 486, 397
152. Unruh, Y.C., Cameron, A.C., Guenther, E. 1998, MNRAS, 295, 781
153. Valenti, J.A., Basri, G., Johns, C.M. 1993, AJ, 106, 2024
154. Ventura, P., Zeppieri, A., Mazzitelli, I., D'Antona, F. 1998, A&A, 331, 1011
155. Vrba, F.J., Chugainov, P.F., Weaver, W.B., Stauffer, J.S. 1993, AJ, 106, 1608
156. Vrba, F.J., Rydgren, A.E., Chugainov, P.F., Shakovskaya, N.I., Weaver, W.B. 1989, AJ, 97, 483
157. Walker, M.F. 1972, ApJ, 175, 8
158. Walker, M.F. 1983, ApJ, 271, 642
159. Walter, M.F. 1986, ApJ, 306, 573
160. Walter, F.M., Brown, A., Mathieu, R.D. Myers, P.C., Vrba, F.J. 1988, AJ, 96, 297
161. Wolf, B., Appenzeller, I., Bertout, C. 1977, A&A, 58, 163
162. Yi, I., 1994, ApJ, 428, 760

ANNEX 1: Properties of T Tauri Stars in Taurus-Auriga

HBC	name	RA (2000)	Dec (2000)	V	K	$v \sin i$ (km/s)	P_{rot} (d)	Sp.Ty.	W(Ha) (Å)	Type	sep. ($''$)	p.a. (o)	ratio @K	1.3mm (mJy)	M_{disk} ($M_\odot$)	log $\dot{M}_{acc}$ ($M_\odot/yr$)
351	034903+2431	3 52 02.3	+24 39 51	12.26	9.2	29	<3.5	K5	1.6	wt	0.61	317	0.22	<14		
352/353	035120+3154	3 54 29.4	+32 03 02	11.8/12.4	9.6/9.9			G8/K0	3/2	-/wt	8.7	71	0.77	<12/<14		
354	035135+2528NW	3 54 35.6	+25 37 12	13.79		<10		K3	hk					<16		
	SAO 76411	4 02 53.5	+22 08 12	8.85				G0		wt				<14		
355/354	035135+2528	3 54 35.9	+25 37 09	12.7/13.9	10.3/11.1			K0/K2		wt	6.3	298	0.46			
356/357	V1067 Tau NS	4 03 14.1	+25 53 00	12.91	10.2	>75		K2	0.9/1.8	?/wt	2			<16		
358	040047+2603W	4 03 49.2	+26 10 54	15.2	9.4			M3	13	wt	1.58	226	0.60			
359	040047+2603E	4 03 50.9	+26 10 55	14.17		<10		M2	2.4	wt				<13		
	SAO 76428	4 04 28.5	+21 56 04	9.3				F8		wt				<14		
360/361	040142+2150	4 04 39.3	+21 58 20	14.9/15.1	10.0/10.1			M3/M3	10/8	wt	7.2	65	0.89	<9/<26		
362	040234+2143	4 05 30.9	+21 51 11	14.67		14		M2	4.0	wt				<14		
365	V1095 Tau	4 13 14.2	+28 19 11	13.72		23		M4	4	wt				<14		
366n	V1096 Tau	4 13 27.2	+28 15 57	13.52:				M0	3	wt				<14		
367	V773 Tau	4 14 12.9	+28 12 12	10.62	6.5	55	3.43	K3	4	wt	0.112	295	0.47	42v	-	
23n	FM Tau	4 14 13.5	+28 12 50	14.22				M0	71	tt				31	<50	-8.45
24	FN Tau	4 11 08.6	+28 20 27	14.95				M5	25	tt				31	40	
25n	CW Tau	4 14 17.0	+28 10 59	12.36		36		K3	135	tt				96	<150	
368	V1098 Tau	4 14 48.0	+27 52 35	12.08	7.5	22	7.2	M1	2.5		0.491	77	0.96	<14		
26	FP Tau	4 11 43.5	+26 38 56	13.90		27		M4	38	tt				<50	<250	
369	FO Tau	4 14 49.6	+28 12 27	15.0:	8.1			M2	117	tt	0.166	182	0.65	<14	<17	-7.50
27	CX Tau	4 11 44.0	+26 40 42	13.72		20		M2.5	20	tt				<40	<110	-8.97
370	V1068 Tau	4 16 28.1	+28 07 36	12.54		26	3.37	K7:	5	wt				<14		
28	CY Tau	4 14 27.7	+28 13 29	13.33		10	7.5:	M1	70	tt				133	7000	-8.12
371	LkCa 5	4 17 39.0	+28 33 02	13.56		38:		M2	4	wt				<14		
29	V410 Tau	4 18 31.1	+28 27 16	10.82	7.5	71	1.87	K7	3v	wt	0.123	218	0.16	<30		
30n	DD Tau	4 18 30.6	+28 16 40	14.11	7.9			M1	182	tt	0.56	186	0.52	17	09	-8.39
31n	CZ Tau	4 15 25.6	+28 09 44	15.33	9.3			M1.5	4	tt	0.33	84	0.46	<30	<30	-9.35
372	041529+1652	4 18 21.4	+16 58 46	13.26		<10		K5	hk					<14		
374n	V1023 Tau	4 18 47.0	+28 20 08	12.73:		13		K7	3	wt				<25		
375	CoKu Tau/1	4 18 51.5	+28 20 28	19.3:				?	70					<12		
376	041559+1716	4 18 51.6	+17 23 15	12.28		68		K7	0.7	wt				<14		
377	FQ Tau	4 16 06.4	+28 22 21	15.6:	9.3			M2	114	tt	0.79	69	0.90	<40	<260	-6.45
32	BP Tau	4 19 15.8	+29 06 27	12.09		7.8	7.6	K7	40	tt				37	<110	-7.54
378	V819 Tau	4 19 26.4	+28 26 14	13.24		<15	5.6	K7	1.7	wt				34	320	
	FR Tau	4 19 35.5	+28 27 23	16.3										<15		
379	V1070 Tau	4 19 41.3	+27 49 39	12.6	8.3	12.9	5.64	K7	4	wt	1.05	25	0.56	<24		
	J2 157	4 20 52.6	+17 46 41							tt				<14		
33	DE Tau	4 21 54.2	+27 55 03	13.00		10	7.6	M2:	54	tt				36	70	-7.58
34n	RY Tau	4 21 57.4	+28 26 36	10.01		52		K1	20v	tt	0.02	317		229	390	
380	HD 283572	4 21 58.9	+28 18 06	9.04		>75	1.55	G5	abs	su				<15		
381n	FS Tau B	4 22 00.9	+26 57 38					?	pr	tt				134	>1700	
382	V1071 Tau	4 22 03.1	+28 25 39	13.47		60:		M3,4	6	tt				<12	-	
383n	FS Tau	4 22 02.1	+26 57 33	15.71	7.3			M1	57	tt	0.265	60	0.12	<35	<30	-8.09
35n	T Tau	4 21 59.4	+19 32 06	9.90	5.4	20	2.8	K1	38	tt	0.71	176	0.09	280	160	
	FU Tau	4 20 33.3	+24 56 08	15.1										<35	<80	
	GT Tau	4 20 34.2	+24 48 22	14.4										<35		
384	FT Tau	4 23 39.2	+24 56 15	14.1				cont	pr	tt				130	340	
	J4423	4 21 40.3	+26 54 54							wt				<11		
385	IP Tau	4 24 57.1	+27 11 58	12.99		<11	3.25	M0:	11					16	48	-9.10
	J4872	4 22 13.8	+26 11 02	13.1				K7?		wt				<14		
386	FV Tau	4 26 53.6	+26 06 55	15.4:	7.5			K5	23	tt	0.73	92	0.64	15	6	-6.23
387n	FV Tau/c	4 26 54.4	+26 06 52	17.2:	8.5			M3	29	tt	0.74	293	0.17	<16		
36	DF Tau	4 27 02.8	+25 42 22	11.49	6.8	16	8.5	M0.5	60	tt	0.088	329	0.47	<25	<100	-6.91
37n	DG Tau	4 27 04.7	+26 06 17	12.01		22	6.3	cont.	113	tt				443	410	
388	V1072 Tau	4 27 10.6	+17 50 44	10.34		16	2.74	K1	hk	wt				<16		
	J 507	4 26 16.3	+26 27 09							wt				<14		

HBC	name	RA (2000)	Dec (2000)	V	K	v sin(i) (km/s)	P_{rot} (d)	Sp.Ty.	W(Ha) (Å)	Type	sep. ($''$)	p.a. (o)	ratio @K	1.3mm (mJy)	M_{disk} ($M_\odot$)	log $\dot{M}_{acc}$ ($M_\odot/yr$)
389n	GV Tau	4 26 21.9	+24 26 30	17.2:	7.0			K3	pr		1.21	355	0.13	116	17	
	FW Tau	4 29 29.6	+26 16 54	17.1(B)	9.2			M3-5	17		0.16	160	1.0	<15	<460	
38	DH Tau	4 26 37.1	+26 26 29	13.92		10.5	7.2	M1	53	tt				53	<170	-8.30
39	DI Tau	4 26 38.0	+26 26 20	12.86	8.4	11	7.5	M0	2	wt	0.12	294	0.13	<35	<110	-8.75
41	IQ Tau	4 26 47.7	+26 00 16	13.30		11.5	6.25	M0.5	7.8	tt				87	400	-7.55
42/43	UX Tau BA	4 27 09.6	+18 07 21	13.7/11.4	8.9/7.7			M2/K5	8/20		5.9	269	0.29	63	65	
43	UX Tau AC	4 27 10.0	+18 07 21	11.4/15.1(R)	7.7/10.5	27	2.7	K5	20	wt	2.7	181	0.07	63	65	
	ZZ Tau B	4 27 14.6	+24 33 02							wt				<20		
44	FX Tau	4 30 26.9	+24 26 35	13.90	8.1	10		M1	10	tt	0.91	292	0.55	<30	<50	-8.65
45	DK Tau	4 30 44.2	+26 01 24	12.40	7.0	11	8.4	K7/K7	19/34	tt	2.53	115	0.30	35	50	-7.42
46	ZZ Tau	4 27 49.3	+24 35 57	14.34	8.5			M3:	15	tt	0.029^{l}	-	0.44	<15	<140	
	JH 56	4 31 14.4	+27 10 19	12.63						wt				<19		
47	V927 Tau	4 28 22.4	+24 04 30	14.63	8.7	19		M5.5	4.7	tt	0.30	290	0.73	<20	<120	
392	V1074 Tau	4 31 27.2	+17 06 25	12.53		17	3.38	K5	0.2	wt				<18		
393n	L1551/IRS 5	4 31 33.6	+18 08 15					K2		?				1276	370	
394	LkHa 358	4 28 42.2	+18 07 21	19.0:				M5.5	47					32	>31	
49n	HL Tau	4 31 38.4	+18 13 59	14.57				K7,M2?	55:	tt				879	1000	
50	XZ Tau	4 31 40.0	+18 13 58	13.30	7.1		2.6:	M3	274	tt	0.311	153	0.51	14	03	
48	HK Tau	4 28 48.9	+24 17 56	15.75	8.7/11.8	22		M0.5	29	tt/tt	2.4	175	0.06	41	50	
	J 665	4 28 55	+25 37 08							wt				<28		
51/395	V710 Tau	4 31 57.8	+18 21 37	14.2/14.4	8.6/8.6	17		M0.5/M2	89/11	tt/wt	3.24	357	0.83	71	540	
396	V806 Tau	4 32 15.7	+24 29 02	17.7:				cont	88	tt				124	140	
397	V1075 Tau	4 32 09.3	+17 57 23	12.06		27	2.43:	K7	0.5	wt						
398	V928 Tau	4 32 18.8	+24 22 28	13.7:	8.0	25		M0.5	1.2	wt	0.165	125	0.60	<11		
399	V827 Tau	4 32 14.6	+18 20 15	12.18		18.5	3.75	K7,M0	1.8	wt				<19	<120	
400	V826 Tau	4 29 22.0	+17 55 19	12.11		4.2	3.7	K7,M0	1.6	wt				<15	<450	
401	FY Tau	4 32 30.5	+24 19 58	15.4:				K7	59	tt				16	30	-7.41
402	FZ Tau	4 29 30.1	+24 13 44	15.0:				cont	204	tt				23	40	
54	GG Tau Aa	4 29 37.1	+17 25 22	12.24	7.5	10	10.3	M0	54	tt	0.288	3	0.25	593	290	-7.76
	GG Tau Bb	4 29 *	+17 25	17.3	10.0			M5	83	tt	1.4	135	0.19			
52/53	UZ Tau ew	4 32 43.1	+25 52 31	13.1/13.7	8.1/7.5	14/16		M2/M3	41/79	tt	3.78	273	0.49	172	540	
53	UZ Tau w	4 32 42.8	+25 52 32	13.7	7.5	16		M3	79	tt	0.360	359	0.46	172		
	JH 112	4 32 49.1	+22 53 03	15.54						tt				<18		
403	V1076 Tau	4 32 43.8	+18 02 58	13.22		11.5	6.20	K7	0.7	wt				<23		
55	GH Tau	4 33 06.1	+24 09 45	12.95	7.8	28:		M1.5	15	tt	0.314	299	0.56	<30	24	-7.92
404	V807 Tau S	4 33 06.6	+24 09 56	11.3	8.3			M0	13	tt	0.023^{l}	-	1.0	17	24	
404	V807 Tau NS	4 33 06.6	+24 09 56	11.3	7.0			M0	13	tt	0.375	330	0.37	17		
405	V830 Tau	4 30 08.3	+24 27 27	12.21		29	2.75	K7,M0	3	wt				<9	<27	
56n	GI Tau	4 33 34.1	+24 21 18	13.01		11	7.2	K7	19	tt				<20	<30	-8.02
59	IS Tau	4 33 36.8	+26 09 50	14.29	8.0			K2	12	tt	0.221	92	0.16	<20	<230	
57n	GK Tau	4 33 34.5	+24 21 07	13.5/17.0	7.6	19	4.65	K7	16	tt	2.4	66	0.03	<21	<30	-8.19
58	DL Tau	4 33 39.1	+25 20 39	13.05		16		cont.	105	tt				230	870	
60/406	HN Tau	4 33 39.3	+17 51 53	14.2/18.1	8.2	53		K5/M4	138/108	tt	3.1	215	0.042	<15	05	-8.89
	IT Tau	4 30 50.5	+26 07 14	14.3	8.2			K0	4.3		2.48	225	0.23	<33	<60	
61	CI Tau	4 30 52.2	+22 44 17	13.09		11		K7	102	tt				190	630	-7.19
62	DM Tau	4 33 48.7	+18 10 12	13.99		<10		M1:	139	tt				109	340	-7.95
	J2-2041	4 33 55.4	+18 38 39							wt				<19		
	JH 108	4 34 10.9	+22 51 45	15.2						wt				<18		
407	V1077 Tau	4 34 18.1	+18 30 07	12.67		12.2	3.32	G8	0.3	wt				<64	-	
408	V1110 Tau	4 34 39.4	+25 01 01	10.37				K0	0.5	?				<19		
63	AA Tau	4 34 55.5	+24 28 54	12.37		11	8.2	K7	37	tt				88	210	-8.48
	V1078 Tau	4 35 14.1	+18 21 37	10.95		<5	3.2	F8		wt				<15		
64	HO Tau	4 32 20.8	+22 26 07	14.4/16:	9.6			M0.5	115	tt	6.9	109		<30	<190	-8.86
409	FF Tau	4 32 20.9	+22 48 17	13.67	8.7			K7	1.4	wt	0.037^{l}	-	0.40	<27	<240	
65	DN Tau	4 32 25.7	+24 08 52	12.36		8	6.0	M0	12	tt				84	270	-8.46

HBC	name	RA (2000)	Dec (2000)	V	K	v sin(i) (km/s)	P_{rot} (d)	Sp.Ty.	W(Ha) (Å)	Type	sep. ($''$)	p.a. (o)	ratio @K	1.3mm (mJy)	M_{disk} ($M_\odot$)	log $\dot{M}_{acc}$ ($M_\odot/yr$)
411	CoKu Tau/3	4 35 41.2	+24 11 08	17.3:	8.2			M1	4.6		2.04	177	0.29	<16	<44	
412	043230+1746	4 35 34.1	+17 51 41	14.12	9.1	<30		M2	9	wt	0.70	68	1.0	<16		
	HQ Tau	4 32 47.4	+22 44 16	12.6	7.4						0.009^l	-	0.14	<45	<110	
66	HP Tau	4 35 53.1	+22 54 24	13.16	7.3	15	5.9:	K3	35	tt	0.017^l	-	0.26	62	50	
414	HP Tau/G3	4 35 53.5	+22 54 10	14.6	8.7			K7	2.0	wt	0.022^l	-	0.40	<17	>37	
415/414	HP Tau G2/G3	4 35 54.1	+22 54 14	11.0/14.6	7.2/8.7	100:/	1.2/	G2/K5	2/2	su	10.0	243	0.24	<14/<17		
416	Haro 6-28	4 35 55.9	+22 54 36	17.3:	9.3			M5	92	tt	0.66	246	0.63	<14	<110	
	FG Tau	4 36 10.1	+24 02 55	16.4(B)				M5						<45	<210	
417	V1115 Tau	4 36 19.1	+25 42 59	13:		22	3.35	M0:	1	wt				<19		
	HD 283759	4 33 47.3	+24 06 58	10.36				F2						<35	<60	
	FI Tau	4 34 11.3	+23 30 16	16.3(B)				M5?		?				<22	<230	
	HT Tau	4 34 46.8	+26 18 01											<50	<460	
67n	DO Tau	4 38 28.6	+26 10 55	14.01				K7	109	tt				136	180	-6.84
418n	HV Tau	4 35 30.9	+26 04 45	14.0:	7.8	14		M1	4.5	wt	0.035^l	-	0.58	40		
418n	HV Tau AB	4 35 30.9	+26 04 45	14.0:	7.8	14		M1	4.5	wt	4.00	45	0.03	40		
	GN Tau	4 39 20.8	+25 45 03	15.7	8.4			cont.	62	tt	0.041^l	-	0.63	<50	<160	
68	VY Tau	4 36 17.4	+22 42 02	13.71	8.8	10	5.37	M0	4.9	tt	0.66	317	0.26	<17	<19	
419	V1079 Tau	4 39 17.8	+22 21 03	12.09		12.5	5.85	K5	13	wt				167	240	-8.87
	JH 223	4 40 49.5	+25 51 20	15.50						wt				<19		
	Haro 6-32	4 41 04.2	+25 57 57											<50		
420	IW Tau	4 41 04.7	+24 51 07	12.5	8.3	7	5.6	K7	4	wt	0.27	177	0.91	<19	<690	
421	CoKu Tau/4	4 41 16.8	+28 40 01	14.9:				M1.5	1.8					<15	<8	
422	LkHa 332/G2	4 42 05.5	+25 22 57	14.9	8.2	20		M0	3.1	wt	0.30	243	0.60	<15	-	
423	LkHa 332/G1	4 42 06.9	+25 23 04	15.4	8.1			M1	3.7		0.215	77	0.56	<14	-	-6.60
69	V955 Tau	4 42 07.7	+25 23 13	14.74	8.0	10		K7,M0	13	tt	0.33	204	0.22	<19	<11	-7.02
70	DP Tau	4 42 37.2	+25 15 31	14.22				M0.5	85	tt				<27	30	-7.88
71	GO Tau	4 43 03.1	+25 20 19	14.89		21		M0	81	tt				83	570	-7.93
72	DQ Tau	4 44 00.0	+16 54 40	13.16				M0,1	113	tt				91	250	-9.40
73/424	V1001 Tau	4 46 59.0	+17 02 39	13.5/14.7	7.5/8.9	10		K7/M1	21/166	tt	2.7	37	0.45	60	170	-7.00
74	DR Tau	4 47 06.3	+16 58 41	11.17v		<10	9.0	cont.	87	tt				159	280	
75	DS Tau	4 44 39.1	+29 19 56	12.4/13.6	8.0/11.3	10		K2/F8	70/0	tt	7.1	294	0.045	25	67	-7.89
76	UY Aur	4 48 35.7	+30 42 14	12.37	7.0			K7	73	tt	0.89	225	0.28	29	9	-7.18
	Haro 6-39	4 52 09.7	+30 37 46											24	50	
425	St 34	4 51 30.3	+17 05 07	13.5:				M	pr					<15		
77	GM Aur	4 51 59.8	+30 17 15	12.03		12	12.0	K3	96	tt				253	600	-8.02
426	V396 Aur	4 55 37.0	+30 17 55	10.85		19	2.24	K0	1:	wt						
79n	SU Aur	4 55 59.4	+30 34 02	8.93		67		G2	4v	su				<30	<30	
427	V397 Aur	4 56 02.2	+30 21 03	11.60		10.4	9.3:	K7	0.7	wt						
429	V836 Tau	5 03 06.6	+25 23 20	13.13		<15	6.78	K7,M0	9v	wt				37	400	
81	RW Aur BC	5 04 37.6	+30 20 14	12.7:	8.7						0.120	111	-	421		
80/81	RW Aur AB	5 04 37.7	+30 20 14	11.1/12.7	6.9	20:/	5.39/	cont.	84v	tt	1.50	258	0.23	421	3	

Columns 1,2 list the star's Herbig and Bell catalogue number and name respectively. **Col. 3,4** are the J2000 coordinates from SIMBAD. **Col. 5,6** are the V and K magnitudes. **Col. 7,8** are vsini and photometric rotation period. **Col. 9-11** give the spectral type, the Hα equivalent width and the type of the star: tt means CTTS, wt means WTTS, su means SU Aur object. **Col. 12-14** contain information on binarity: the projected separation, the apparent position angle, in degrees East of North, and the flux ratio (primary/secondary) in the K-band. A superscript l means lunar occultation. (mostly from Mathieu 1994, ARAA) **Col. 15-16** list the 1.3mm continuum flux and the correspondent disk mass ([12],125]). The last **column, 17**, is the mass accretion rate estimated by [71].